T2R2 東京科学大学 リサーチリポジトリ
Science Tokyo Research Repository

論文 / 著書情報
Article / Book Information

Title	Two auxiliary factors promote Dmc1-driven DNA strand exchange via stepwise mechanisms
Authors	Hideo Tsubouchi, Bilge Argunhan, Kentaro Ito, Masayuki Takahashi, Hiroshi Iwasaki
Citation	Proceedings of the National Academy of Sciences of the United States of America, Vol. 117, No. 22, pp. 12062-12070
Pub. date	2020, 5
DOI	10.1073/pnas.1917419117
Note	This file is author (final) version.

Powered by T2R2 (Science Tokyo Research Repository)

Two Auxiliary Factors Promote Dmc1-Driven DNA Strand Exchange via Stepwise Mechanisms

Hideo Tsubouchi[1,3,*], Bilge Argunhan[1], Kentaro Ito[1], Masayuki Takahashi[2], Hiroshi Iwasaki[1,3]

[1]Institute of Innovative Research, Tokyo Institute of Technology, Tokyo, Japan.

[2]School of Life Science and Technology, Tokyo Institute of Technology, Tokyo, Japan.

[3]Co-corresponding authors.

***Lead contact: htsubouchi@bio.titech.ac.jp**

Classification

BIOLOGICAL SCIENCES, Biochemistry

Keywords

Dmc1; double-stranded break; fission yeast; homologous recombination; Rad51

Author Contributions

H.T. and H.I. conceived the project. H.T., B.A. and K.I. performed all of the experiments and H.T., K.I. and M.T. analyzed the data. H.T., B.A. and H.I. wrote the manuscript with input from the other authors.

Competing Interest Statement

The authors declare no competing interests.

This PDF file includes:

Main Text

Figures 1 to 5

Abstract

Homologous recombination (HR) is a universal mechanism operating in somatic and germline cells, where it contributes to the maintenance of genome stability and ensures the faithful distribution of genetic material, respectively. The ability to identify and exchange the strands of two homologous DNA molecules lies at the heart of HR and is mediated by RecA-family recombinases. Dmc1 is a meiosis-specific RecA homolog in eukaryotes, playing a predominant role in meiotic HR. However, Dmc1 cannot function without its two major auxiliary factor complexes, Swi5-Sfr1 and Hop2-Mnd1. Through biochemical reconstitutions, we demonstrate that Swi5-Sfr1 and Hop2-Mnd1 make unique contributions to stimulate Dmc1-driven strand exchange in a synergistic manner. Mechanistically, Swi5-Sfr1 promotes establishment of the Dmc1 nucleoprotein filament whereas Hop2-Mnd1 defines a critical, rate-limiting step in initiating strand exchange. Following execution of this function, we propose that Swi5-Sfr1 then promotes strand exchange with Hop2-Mnd1. Thus, our findings elucidate distinct yet complementary roles of two auxiliary factors in Dmc1-driven strand exchange, providing mechanistic insights into some of the most critical steps in meiotic HR.

Significance statement

Homologous recombination (HR) is highly induced during meiosis as it plays an essential role in segregating chromosomes at the first division of meiosis. Dmc1 is the major enzyme responsible for homology searching and strand exchange in meiosis. However, in the cell, Dmc1 cannot function without two major auxiliary factors, Hop2-Mnd1 and Swi5-Sfr1. How these auxiliary factors collaborate to facilitate Dmc1's activity remained elusive. Here, we demonstrate that Hop2-Mnd1 allows Dmc1 to access and initiate strand invasion into homologous dsDNA while Swi5-Sfr1 acts to stabilize Dmc1 binding to single-stranded DNA and promote strand exchange with Hop2-Mnd1. Thus, our findings provide fundamental insights into the mechanism of meiotic HR, which is central to inheritance and evolution.

Introduction

Homologous recombination (HR) is critical for accurately repairing DNA double-strand breaks and thus maintaining genome integrity (1). Defective HR progressively deteriorates the quality of the genome, eventually leading to the occurrence of cancer (2). HR also plays an essential role in meiosis where it ensures accurate segregation of homologous chromosomes (3, 4).

Rad51 and Dmc1 are eukaryotic orthologs of the prokaryotic homologous recombinase RecA (5, 6). Unlike Rad51, which contributes to both mitotic and meiotic recombination, Dmc1 functions only during meiosis. Both Rad51 and Dmc1 bind single-stranded DNA (ssDNA) that is exposed as DSB ends are resected and form a right-handed helical structure called the presynaptic filament. Formation and stability of this structure is critical for Rad51/Dmc1 to conduct efficient homology searching and strand exchange (7).

Rad51/Dmc1 require a number of auxiliary factors in order to function efficiently in vivo (8, 9). Among these, a group of proteins called recombination mediators facilitate the loading of Rad51/Dmc1 onto nascent ssDNA preoccupied by replication protein A (RPA), a eukaryotic ssDNA binding protein. The Swi5-Sfr1 complex in the fission yeast *Schizosaccharomyces pombe* (Mei5-Sae3 in *Saccharomyces cerevisiae*) has been characterized as an auxiliary factor that stimulates Dmc1/Rad51 (10–15), and has also been shown to promote the formation of interhomolog Holliday junctions/crossovers during meiosis (16, 17). Swi5-Sfr1 is widely conserved in eukaryotes (18–20). Biochemically, Swi5-Sfr1 stabilizes Rad51/Dmc1 presynaptic filaments and stimulates their ATPase activity (15, 21–24).

The Hop2-Mnd1 complex is another widely conserved auxiliary factor of Dmc1

(25–30). The fission yeast ortholog is named Meu13-Mcp7, but Hop2-Mnd1 will be employed throughout because it is the more commonly used name. Hop2-Mnd1 specifically stimulates Dmc1 in fungi and plants (20, 31–36), while it can also promote Rad51 activity in mice and humans (37–40). Although Hop2-Mnd1 is generally believed to function as an obligate heterodimer, Hop2 may have an Mnd1-independent function in mice (41). Hop2-Mnd1 was proposed to help Rad51/Dmc1 to capture target double-stranded DNA (dsDNA) during the homology search and also stabilize Rad51/Dmc1 presynaptic filaments (37, 40). Cytological observations in budding yeast revealed an aberrant but robust accumulation of Dmc1 and Rad51 on meiotic chromosomes in the absence of Hop2/Mnd1 (26, 29). In stark contrast, the chromosomal localization of Dmc1 was completely lost in cells lacking Mei5-Sae3 (19, 20). These results suggested that Hop2-Mnd1 and Swi5-Sfr1 differentially regulate Dmc1, although the differences and interplay between these two complexes remained largely unexplored.

Here, we employed a biochemical approach to elucidate the mechanisms of Dmc1 activation by its two major auxiliary factors. We demonstrate that Hop2-Mnd1 is essential for the Dmc1 presynaptic filament to invade into homologous dsDNA. The function of Swi5-Sfr1 is distinct, as it acts to stabilize Dmc1 binding to single-stranded DNA and, together with Hop2-Mnd1, promotes strand exchange. Thus, Hop2-Mnd1 defines a critical, rate-limiting step in initiating strand exchange by allowing Dmc1 presynaptic filaments to invade into duplex DNA, effectively serving as an initiator of strand exchange in meiotic HR.

Results

Hop2-Mnd1 Promotes Hyper Joint Molecule Formation

The fission yeast Hop2-Mnd1 complex was purified, along with other necessary proteins (*SI Appendix*, Fig. S1A), and its effect on Dmc1-driven strand exchange was tested in an assay that employs 5.4 kb circular ssDNA (css) and homologous linear dsDNA (lds; Fig. 1A). Pairing between css and the complementary strand of lds produces an intermediate (joint molecule, JM), and once the reaction is complete, a nicked circular DNA (nc) as the final product. Hop2-Mnd1 promoted Dmc1 activity at concentrations as low as 0.13 μM (1/40th the concentration of Dmc1), as demonstrated by the production of JM and nc (Fig. 1B). Interestingly, at higher concentrations, JMs of higher molecular weight (referred to as hyper JMs hereafter, denoted with asterisks in Fig. 1B) appeared with some signal observed in the well. The amount of nc declined as hyper JMs increased, suggesting that most DNA substrates are incorporated into strand exchange reactions that are never completed. The inclusion of ATP, Dmc1 and Hop2-Mnd1 is indispensable for formation of hyper JMs and nc (*SI Appendix*, Fig. S1B). We confirmed that the smear corresponding to hyper JMs is not an artifact caused by insufficient proteolysis before agarose gel electrophoresis, which could lead to a similar retardation in the mobility of DNA (*SI Appendix*, Fig. S1C). Hyper JMs are likely to be comprised of css and lds molecules that have undergone incomplete strand exchange because heat treatment resolved most of the JM species, leading to an increase in nc and lds (*SI Appendix*, Fig. S1D). Hyper JM structures might be produced via strand invasion of a single css into multiple lds molecules (42), thus forming a high-molecular weight DNA network (43).

Mechanistically, mouse Hop2-Mnd1 was proposed to stimulate human

Rad51/Dmc1 by enhancing the ability of presynaptic filaments to capture dsDNA (37, 41, 44). This property was tested using fission yeast Hop2-Mnd1. The assay employed css annealed to a biotin-conjugated oligonucleotide, which allows precipitation of the css using streptavidin-coated magnetic beads (*SI Appendix*, Fig. S2A). css was initially incubated with Dmc1 in the presence of AMP-PNP to form stable presynaptic filaments. The reaction was then supplemented with Hop2-Mnd1. Either homologous (PhiX174) or nonhomologous (pBluescript) linear dsDNA was added to the reaction and the fraction of dsDNA associated with css (pellet, P) was separated from the rest (supernatant, S) using magnetic beads. dsDNA efficiently precipitated with css only when the reaction contained both Dmc1 and Hop2-Mnd1 (*SI Appendix*, Fig. S2B). PhiX174 and pBluescript were pulled down to a similar extent, indicating that homology between css and dsDNA is not necessary for dsDNA to be pulled-down. These results strongly argue that, much like its mouse counterpart, fission yeast Hop2-Mnd1 facilitates dsDNA capture by Dmc1 presynaptic filaments.

Next, we decided to closely examine the biochemical similarities/differences between Hop2-Mnd1 and Swi5-Sfr1, another major auxiliary factor of Dmc1. Time-course analysis of Dmc1-driven strand exchange revealed that, in the presence of Hop2-Mnd1, the majority of lds is converted into a wide range of JMs accounting for ~70% of total DNA by 20 min, with the sum of nc and JMs plateauing at 60 min (Fig. 1C). In contrast, the disappearance of lds was more gradual in the reaction containing Swi5-Sfr1, and the sum of nc and JMs progressively increased up until 120 min. Thus, strand exchange stimulated by Hop2-Mnd1 is much quicker than that stimulated by Swi5-Sfr1. The apparent difference in the stimulation of Dmc1 by these two auxiliary factors prompted us to examine if they act synergistically in this reaction. Indeed, when Hop2-Mnd1 and Swi5-Sfr1 were both incubated with Dmc1 presynaptic

filaments, a more robust production of hyper JMs was seen (Fig. 1D).

Hop2-Mnd1 and Swi5-Sfr1 Noncompetitively Bind Dmc1

We next examined the physical interactions between Hop2-Mnd1 and the other proteins employed here (*SI Appendix*, Fig. S1A). Hexahistidine-tagged Hop2-Mnd1 (6xHis-Hop2-Mnd1) was incubated with either Dmc1 or Rad51, then 6xHis-Hop2-Mnd1 was precipitated with nickel-conjugated beads (*SI Appendix*, Fig. S3A). Dmc1, and to a lesser extent Rad51, was pulled down with Hop2-Mnd1, which is consistent with a previous report (34). Interaction of Hop2-Mnd1 with Swi5-Sfr1 or RPA was barely detectable.

Since Dmc1 can physically bind to both Swi5-Sfr1 (14) and Hop2-Mnd1 (*SI Appendix*, Fig. S3A), we sought to test whether these interactions involve the same site on Dmc1. A competition binding assay was devised where 6xHis-Hop2-Mnd1 and Dmc1 were incubated with increasing amounts of Swi5-Sfr1. As a control, 6xHis-Hop2-Mnd1 and Dmc1 were incubated with various concentrations of untagged Hop2-Mnd1, which should compete with 6xHis-Hop2-Mnd1 for Dmc1 binding. As expected, the presence of untagged Hop2-Mnd1 reduced the pull-down efficiency of Dmc1 by 6xHis-Hop2-Mnd1 in a concentration-dependent manner (*SI Appendix*, Fig. S3B,C). In contrast, the amount of pulled-down Dmc1 was not affected by the presence of Swi5-Sfr1. Furthermore, the amount of Swi5-Sfr1 that was pulled down by 6xHis-Hop2-Mnd1—in the presence of Dmc1—was increased at higher concentrations of Swi5-Sfr1, strongly arguing that these two auxiliary factors bind to different interfaces on Dmc1. This noncompetitive binding is consistent with the synergistic stimulation of Dmc1 by Hop2-Mnd1 and Swi5-Sfr1.

The ability of Hop2-Mnd1 to interact with Rad51 prompted us to examine if it

stimulates Rad51-driven strand exchange. While Swi5-Sfr1 stimulated both Dmc1 and Rad51 (14), Hop2-Mnd1 had little effect on the activity of Rad51 (*SI Appendix*, Fig. S4A). However, mild stimulation of Rad51-driven strand exchange was seen when reactions containing Swi5-Sfr1 were supplemented with Hop2-Mnd1 (*SI Appendix*, Fig. S4B). This suggests that Hop2-Mnd1 can also stimulate Rad51, albeit to a far lesser extent than Dmc1.

End-Dependency for Efficient Strand Exchange Is Bypassed by Hop2-Mnd1

How can Dmc1, when stimulated by Hop2-Mnd1, produce JMs more robustly and quickly than Swi5-Sfr1 (Fig. 1C)? One possibility is that Hop2-Mnd1 allows Dmc1 presynaptic filaments to access lds with more freedom. We hypothesized that Swi5-Sfr1-stimulated Dmc1 can only access lds at its ends, while Hop2-Mnd1 also permits internal entries. The lds substrate used so far has ends created by ApaLI, which generates 5' overhangs. To examine the relationship between strand exchange and dsDNA ends, lds with various ends were created (Fig. 2A). lds prepared with XhoI, like ApaLI, was utilized efficiently by Dmc1 in the presence of Swi5-Sfr1 (Fig. 2B). When lds with 3' overhangs was prepared by PstI or AatII, strand exchange was substantially reduced, more so for AatII than PstI. Virtually no strand exchange was seen when lds was prepared with StuI, suggesting that blunt-ends hindered strand exchange. However, with SspI-digested lds, which also has blunt ends, some products were seen. Since the SspI-created ends are A/T-rich, how easily the duplex around an end is separated could also be an important parameter. Nonetheless, these results indicate that Swi5-Sfr1-stimulated strand exchange by Dmc1 relies heavily on the ends of lds. In sharp contrast, robust JM and nc formation was seen in Hop2-Mnd1-stimulated reactions containing lds substrates prepared with any of the 6

different restriction enzymes (Fig. 2). Thus, Hop2-Mnd1 nullifies the end dependency in Dmc1-driven DNA strand exchange.

The Dmc1 Presynaptic Filament Is Not Stabilized by Hop2-Mnd1

Swi5-Sfr1 is an auxiliary factor with "mediator" activity for Dmc1 (15), meaning that it can facilitate the displacement of ssDNA-bound RPA by Dmc1 (45). We examined if Hop2-Mnd1 also has mediator activity. The strand exchange assay used above was modified so that ssDNA was coated with RPA first, followed by addition of other proteins and lds. Swi5-Sfr1 stimulated Dmc1 in a concentration-dependent manner (Fig. 3A). Although some products were obtained with Hop2-Mnd1 in a concentration-independent manner, the yield was substantially reduced, with a ~5-fold reduction in the final products. This indicates that Hop2-Mnd1 does not possess robust mediator activity for Dmc1.

Next, the stabilizing effect of Hop2-Mnd1 on the Dmc1 presynaptic filament was examined using the RPA chase assay (Fig. 3B). A biotin-conjugated oligonucleotide was first annealed to css, and this was then incubated with Dmc1 to form the presynaptic filament. Subsequently, reactions were supplemented with either Swi5-Sfr1 or Hop2-Mnd1, followed by the addition of RPA to challenge the presynaptic filaments by competing for css binding. css was then precipitated by streptavidin-coated magnetic beads and the amount of css-bound Dmc1 was examined. Stable Dmc1 filaments remain associated with css, whereas unstable filaments allow RPA to bind the css, leading to a reduction in the amount of css-bound Dmc1. Inclusion of these auxiliary factors had little effect on the binding of Dmc1 to css in the absence of RPA (*SI Appendix*, Fig. S5A). When preincubated with Swi5-Sfr1, Dmc1 effectively resisted displacement by RPA (Fig. 3C, compare lane 1

with 4,5). Without Swi5-Sfr1, the amount of Dmc1 bound to css was drastically reduced, even in the presence of Hop2-Mnd1, and this was accompanied by an increase in css-bound RPA (Fig. 3C, lanes 1-3). Thus, unlike Swi5-Sfr1, Hop2-Mnd1 does not stabilize the Dmc1 presynaptic filament against displacement by RPA.

In order to more directly assess Dmc1 filament stability, the fluorescence anisotropy assay was employed. In this assay, fluorescently labelled ssDNA (72-mer oligo dT) was preincubated with Dmc1, then either Swi5-Sfr1 or Hop2-Mnd1 was added. Next, the reaction was diluted and the change in fluorescence anisotropy was monitored over time. Upon dilution, anisotropy values showed a gradual decline (Fig. 3D), indicating that the mass associated with ssDNA, primarily contributed by Dmc1, was decreasing. This decline was less steep when Swi5-Sfr1 was included: at 0.6 μM of Swi5-Sfr1 (1/5th the concentration of Dmc1), k_{off} was reduced by 8.9-fold (*SI Appendix*, Fig. S5B). In sharp contrast, the inclusion of Hop2-Mnd1 had no obvious effect on anisotropy, indicating that Swi5-Sfr1 is an efficient stabilizer of the Dmc1 presynaptic filament while Hop2-Mnd1 is not.

The results thus far uncovered the attributes unique to each auxiliary factor. Swi5-Sfr1 is an efficient mediator/stabilizer of Dmc1 filaments, whereas Hop2-Mnd1 allows Dmc1 presynaptic filaments to engage dsDNA in the strand exchange reaction irrespective of the donor's ends. To examine if these unique attributes function in a collaborative manner, a condition requiring both activities was employed by precoating css with RPA and utilizing lds with StuI-digested ends. Hyper JMs were only produced when both Swi5-Sfr1 and Hop2-Mnd1 were included in the reaction, demonstrating that these factors stimulate Dmc1-driven strand exchange in a complementary fashion (Fig. 3E). We note that this synergism was only observed for hyper JM formation, while the levels of nc was actually reduced (also seen in Fig. 1B

and 1D). This may be due to unproductive strand invasion events wherein one css invades into multiple lds molecules, some of which may already be engaged in reactions with other css molecules. The formation of such DNA networks would be expected to hinder the strand transfer reactions—which specifically drive the conversion of JMs into nc—for all DNA molecules involved.

Two Auxiliary Factors Play Distinct but Complementary Roles to Achieve Efficient Strand Exchange

HR in vivo is initiated at a DSB that is resected to form 3'-ended ssDNA at its ends, which searches for homology embedded somewhere within intact dsDNA. This homology is unlikely to be exposed at or near a DSB. Thus, we introduced a set of substrates that better mimic the strand exchange that occurs in vivo. A reasonably long (1.1 kb) linear ssDNA (lss) was employed as the recipient molecule (the molecule which incurs a DSB is termed recipient because it receives information from a donor dsDNA once homology is identified). As a donor substrate, one assay employed linear dsDNA (3.7 kb) with the region homologous to the ssDNA embedded near the middle of the molecule (Fig. 4A, left panel). Another assay employed nicked circular dsDNA (Fig. 4A, right panel), which lacks DNA ends, as a donor. With these two sets of substrates, ssDNA was preincubated with Dmc1, followed by further incubation with RPA and dsDNA with or without auxiliary factor(s). In both cases, Hop2-Mnd1 stimulated product formation, which was further promoted by the presence of Swi5-Sfr1, while Swi5-Sfr1 on its own barely stimulated Dmc1 (Fig. 4B). When ssDNA was precoated with RPA, efficient product formation was seen only when the reaction was supplemented with both Hop2-Mnd1 and Swi5-Sfr1 (Fig. 4C), further highlighting the distinct but complementary roles played by these two auxiliary

factors in stimulating Dmc1-driven strand exchange.

We also examined the effect of heterology (70 bp), located at either the 5'-, 3'- or both ends of lss (Fig. 5A). Products were practically undetectable without any auxiliary factors and the inclusion of just Swi5-Sfr1 had a marginal effect on product formation. The inclusion of Hop2-Mnd1 resulted in reasonably efficient product formation when lss had at least one end free of heterology, achieving a yield of 40-50%, while the presence of heterology at both ends substantially reduced the reaction efficiency (~10%). When both Hop2-Mnd1 and Swi5-Sfr1 were added to the reaction, the lss species with heterology at either end and those without any heterology achieved even higher yields (70-80%). Strand exchange was much less efficient when both ends of lss contained heterology (< 40%). Taken together, we conclude that homology exposed at ssDNA ends is important, but not essential, for strand exchange.

Discussion

Here, we closely examined the functional relationship between two major auxiliary factors of Dmc1 by reconstituting Dmc1-driven strand exchange reactions in vitro. Previous work proposed that mouse Hop2-Mnd1 stabilizes presynaptic filaments of human Rad51 and Dmc1, as well as facilitating the capture of dsDNA by these presynaptic filaments (37, 40). We asked how the action of Dmc1-driven strand exchange could be collaboratively promoted by Hop2-Mnd1 and Swi5-Sfr1, another major auxiliary factor of Dmc1.

Hop2-Mnd1 and Swi5-Sfr1 share a number of biochemical properties. Hop2-Mnd1 binds both dsDNA and ssDNA, with a conditional preference for dsDNA (when the substrate is relatively short, ~100 bp) (46, 47). Swi5-Sfr1 also binds both ssDNA and dsDNA, although a potential binding preference has not been well explored (21, 48, 49). Similarity is not restricted to their biochemical properties; the heterodimeric structure of both Hop2-Mnd1 and Swi5-Sfr1 is mediated by crescent-like leucine zippers, and the resultant parallel coiled-coils can be modeled to fit into the helical groove of the Dmc1/Rad51 filament in both cases (46, 49).

Based on these previous findings, we investigated how these two auxiliary factors contribute to strand exchange driven by *S. pombe* Dmc1. First, we found that Swi5-Sfr1 plays the primary role in establishing Dmc1 presynaptic filaments onto RPA-coated ssDNA (Fig. 3A-D). Then, while both Hop2-Mnd1 and Swi5-Sfr1 are strong activators of Dmc1 strand exchange, Hop2-Mnd1 is exclusively required for Dmc1 presynaptic filaments to access homology within continuous dsDNA (Fig. 2B and 4B). During invasion of ssDNA into homologous dsDNA, the presence of homology at the ssDNA end is a critical determinant for strand exchange efficiency

since the ssDNA substrate with heterology at both ends was utilized relatively poorly in this reaction (Fig. 5B). Importantly, even when the homology is embedded internally in dsDNA, Swi5-Sfr1 can activate strand exchange when acting together with Hop2-Mnd1 (Fig. 4C).

The findings presented here have been combined with previous key findings into a model (Fig. 5D). First, the DSB end is resected to expose 3'-ended ssDNA, which is initially occupied by RPA. This could prevent unfavorable binding of HR proteins such as Hop2-Mnd1 and Rdh54/Tid1 to ssDNA (50) (Fig. 5D-a.). Swi5-Sfr1 primarily promotes replacement of RPA with Dmc1, resulting in formation of the Dmc1 presynaptic filament (Fig. 5D-b.). Results from budding yeast suggest that interactions between Rad51, Mei5-Sae3 and RPA may also play an important role during this step (50, 51). The subsequent invasion of the Dmc1 filament into homologous dsDNA and establishment of the initial annealing of ssDNA is promoted exclusively by Hop2-Mnd1, leading to the initiation of strand exchange (Fig. 5D-c.). This occurs preferentially (but not exclusively) at the 3'-end of the ssDNA molecule (compare 1 and 3 in Fig. 5B and C). Hop2-Mnd1 is a V-shaped heterodimer with two juxtaposed winged-helix domains located near each subunit's N-terminus (46). These domains provide the dsDNA binding activity that is likely involved in promoting the capture of dsDNA by Dmc1 filaments (44, 52). It was proposed that the binding of dsDNA by Hop2-Mnd1 perturbs dsDNA base pairing (46), which would be conducive to strand invasion. Additionally, Hop2-Mnd1 binding to the Dmc1 filament could induce a conformational change in Dmc1 that has a stimulatory effect on strand invasion (53). Following strand invasion, Swi5-Sfr1 and Hop2-Mnd1 likely promote further extension of the heteroduplex by stimulating Dmc1-driven strand transfer (Fig. 5D-d.). This could be achieved solely through stabilization of the Dmc1 filament. It is

also possible that Swi5-Sfr1 functions at this stage similarly to how it stimulates the synaptic phase of Rad51-driven strand exchange in an ATP-hydrolysis-dependent manner, thus fulfilling more than just a filament stabilization role (22). The stimulation of Dmc1's ATPase activity by Swi5-Sfr1 is consistent with this possibility (14). Heteroduplex extension and further branch migration are likely to also involve Rdh54/Tid1 (54–57).

What exactly does the initiation of strand exchange entail at the molecular level? It is noteworthy that in strand exchange assays employing linear ssDNA and dsDNA (linear or nicked circular) (Fig. 4B), or PhiX174-based css and blunt-ended (StuI-ended) dsDNA (Fig. 2B), Swi5-Sfr1 could only promote strand exchange in the presence of Hop2-Mnd1. Importantly, when the ends of donor dsDNA had ssDNA overhangs in the PhiX174-based system, this requirement for Hop2-Mnd1 was bypassed (i.e., Swi5-Sfr1 could stimulate strand exchange without Hop2-Mnd1, Fig. 2B). Thus, we speculate that the strand invasion promoted by Hop2-Mnd1 occurs through a related mechanism involving the exposure of ssDNA. The activity of Hop2-Mnd1 could result in the local melting of dsDNA, allowing the ssDNA within the Dmc1 filament to establish base pairing with a few nucleotides of the complementary strand. This nascent D-loop may then be acted on by Swi5-Sfr1, which could promote further strand transfer. In this sense, the action of Hop2-Mnd1 can be defined as a step in Dmc1-driven DNA strand exchange after which Swi5-Sfr1 is able to promote progression of the reaction. As such, the initiation of strand exchange represents a critical, rate-limiting step that requires the activity of Hop2-Mnd1, and consequently enables Swi5-Sfr1 to potentiate Dmc1.

Hop2-Mnd1 is unique among auxiliary factors for RecA homologs in that a severe defect in meiotic DSB repair is observed in its absence despite the robust

accumulation of Rad51 and Dmc1 on meiotic chromosomes in many different organisms (26, 29, 58–60). This phenotype is consistent with an essential role for Hop2-Mnd1 in initiating strand exchange. Furthermore, the apparently robust localization of Rad51/Dmc1 to meiotic chromosomes in the absence of Hop2-Mnd1 argues that presynaptic filament formation/stabilization is not the primary role of Hop2-Mnd1. In contrast, the inability of Dmc1 to localize to chromosomes in the absence of Mei5-Sae3 (19, 20) suggests that Mei5-Sae3 is important for Dmc1 filament formation/stabilization. These cytological observations are in complete agreement with the biochemical results presented here (Fig. 3).

Dmc1 and Hop2-Mnd1 belong to a core group of meiotic genes that are thought to have existed since the origin of meiosis and evolved together thereafter (61). In *S. cerevisiae*, Hop2-Mnd1 functions exclusively within meiosis just like Mei5-Sae3. Although Mei5-Sae3 can physically interact with Rad51, its ability to stimulate strand exchange is limited to Dmc1 (48). In *S. pombe* and mice, however, Swi5-Sfr1 also has a mitotic role in promoting Rad51-dependent DNA repair (10, 18). Interestingly, although exclusively meiosis-specific in budding and fission yeasts, *S. pombe* Hop2-Mnd1 can bind and weakly potentiate Rad51 (*SI Appendix*, Fig. S4B) while *S. cerevisiae* Hop2-Mnd1 does not seem to even associate with Rad51 (31). Furthermore, Hop2-Mnd1 is produced in somatic cells of higher eukaryotes (30, 62, 63) and is involved in alternative lengthening of telomeres in humans (64). Given the fact that organisms lacking Dmc1 also lack Hop2 and Mnd1 (e.g., *C. elegans*, *Drosophila* and *Neurospora*), Hop2-Mnd1, which used to act exclusively with Dmc1, might have acquired the novel function of activating Rad51 as it was also produced in vegetative cells throughout the course of evolution. *S. pombe* may represent an intermediary where Hop2-Mnd1 is in the process of developing the capacity to

stimulate Rad51.

In conclusion, our work highlights the unique attributes of Hop2-Mnd1 and Swi5-Sfr1 in collaboratively and complementarily activating Dmc1-driven strand exchange.

Materials and Methods

Three-Strand Exchange and D-loop Assay

All the reactions were conducted in the scale of 10 µL at 30˚C. The following conditions were employed with PhiX174 substrates unless otherwise stated. Strand exchange buffer (30 mM Tris-Cl [pH 7.5], 120 mM NaCl, 30mM KCl, 3.5 mM $MgCl_2$, 2 mM ATP, 1 mM DTT, 5% glycerol, 8 mM phosphocreatine, 8 units/mL creatine phosphokinase) containing 10 µMnt PhiX174 virion DNA (i.e., css [NEB]) was supplemented with 5 µM Dmc1 or Rad51 and incubated for 5 min. The indicated concentration of auxiliary factor(s), typically 0.25 µM for Hop2-Mnd1 and 0.5 µM for Swi5-Sfr1, was added to the reaction, which was further incubated for 5 min. 1 µM RPA was then added and incubated for 10 min. The strand exchange reaction was started by adding 10 µMnt of linearized dsDNA (lds, PhiX174 RF I DNA [NEB], ApaLI digested unless otherwise stated), which lasted for either 1 h or 2 h (as specified). Strand exchange between css and lds initially produces joint molecules (JMs) as intermediates, which are then converted to nicked circular molecules (nc) and a linear ssDNA upon completion of strand exchange. lss is not visible on the gel because the band overlaps with css (Fig. 1A). In the case of the D-loop system, 5 µMnt linear ssDNA was supplemented with 5 µM Dmc1 and incubated for 10 min. The indicated concentration of auxiliary factor (typically 0.25 µM for Hop2-Mnd1 and 0.5 µM for Swi5-Sfr1), 1 µM of RPA and 5 µMnt nicked circular or linear dsDNA, were then mixed to start the reaction, which lasted for 1 h (or as indicated). In the case of mediator assays using PhiX174 substrates, 10 µMnt of PhiX174 virion DNA (css) was incubated with RPA at 2 µM for 10 min, then mixed with Dmc1, auxiliary factor(s) at 0.25 µM for Hop2-Mnd1 and/or 4 µM for Swi5-Sfr1, and linear PhiX174 RF I DNA

(ApaLI digested unless otherwise stated) at 10 μMnt, which lasted for 1 h. In the case of D-loop mediator assays, 5 μMnt linear ssDNA was supplemented with 2 μM RPA and incubated for 10 min. Then, 5 μM Dmc1, indicated concentrations of auxiliary factor (typically 0.25 μM for Hop2-Mnd1 and 0.5 μM for Swi5-Sfr1), and 5 μMnt nicked circular or linear dsDNA, were then mixed to start the reaction, which lasted for 1 h. At the end of all the reactions described above, 10 μL reactions were subjected to psoralen-UV crosslinking to stabilize labile DNA structures and 2 μL of stop solution was added (30 mM Tris-Cl [pH 7.5], 44 mM EDTA, 3% SDS, 15 mg/mL proteinase K). Following a 5 min incubation, DNA was resolved in 1% agarose gels and stained with SYBR Gold (Thermo Fisher Scientific). Gels were then imaged using a LAS4000 mini (GE Healthcare). Data acquisition and analysis were done as before except FIJI (65) was employed for signal quantification (14, 23). In brief, in the case of PhiX174-based substrates, background was subtracted and the amount of signal for areas corresponding to lds, nc and JM bands was measured with the JM values divided by 1.5 to compensate for the extra signal generated by these three-stranded DNA molecules. The sum of the values was set to 100% and the percentage of total DNA corresponding to nc or JM was calculated. For the total yield, the percentage of DNA corresponding to nc and JM was combined. In the case of the D-loop assay, the sum of the value for dsDNA (nc or lds) and that for the product was set to 100%, and the yield was expressed as the percentage of the product per the sum. The values from three independent experiments were averaged and plotted along with error bars (SD). In *SI Appendix*, Fig. S4B, statistical significance was assessed by a paired t-test.

Data Availability

All relevant data are presented in the manuscript. Requests for reagents or further

information should be directed to H.T. (htsubouchi@bio.titech.ac.jp).

Additional Materials and Methods are in the *SI Appendix*.

Acknowledgements

This study was supported in part by Grants-in-Aid for Scientific Research (B) (18H02371 to H.T.), for Scientific Research (A) (18H03985 to H.I.), for Scientific Research on Innovative Areas (15H059749 to H.I.), and for Young Scientists (B) (17K15061 to B.A.).

References

1. A. Mehta, J. E. Haber, Sources of DNA Double-Strand Breaks and Models of Rec. *Cold Spring Harb. Perspect. Biol.* **6**, 1–19 (2014).
2. R. Prakash, Y. Zhang, W. Feng, M. Jasin, Homologous Recombination and Human Health. *Perspect. Biol.*, 1–29 (2015).
3. N. Hunter, Meiotic Recombination: The Essence of Heredity. *Cold Spring Harb. Perspect. Biol.* **7**, a016618 (2015).
4. M. Petronczki, M. F. Siomos, K. Nasmyth, Un ménage à quatre: the molecular biology of chromosome segregation in meiosis. *Cell* **112**, 423–40 (2003).
5. M. S. Brown, D. K. Bishop, DNA Strand Exchange and RecA Homologs. *Cold Spring Harb. Perspect. Biol.*, 1–30 (2014).
6. J. M. Daley, W. A. Gaines, Y. Kwon, P. Sung, Regulation of DNA Pairing in Homologous Recombination. *Cold Spring Harb. Perspect. Biol.* **6**, 1–15 (2014).
7. J. B. Crickard, E. C. Greene, Biochemical attributes of mitotic and meiotic presynaptic complexes. *DNA Repair (Amst).* **71**, 148–157 (2018).
8. W.-D. Heyer, K. T. Ehmsen, J. Liu, Regulation of Homologous Recombination in Eukaryotes. *Annu. Rev. Genet.* **44**, 113–139 (2010).
9. J. San Filippo, P. Sung, H. Klein, Mechanism of Eukaryotic Homologous Recombination. *Annu. Rev. Biochem.* **77**, 229–257 (2008).
10. Y. Akamatsu, D. Dziadkowiec, M. Ikeguchi, H. Shinagawa, H. Iwasaki, Two different Swi5-containing protein complexes are involved in mating-type switching and recombination repair in fission yeast. *Proc. Natl. Acad. Sci.* **100**, 15770–15775 (2003).

11. Y. Akamatsu, *et al.*, Fission yeast Swi5/Sfr1 and Rhp55/Rhp57 differentially regulate Rhp51-dependent recombination outcomes. *EMBO J.* **26**, 1352–1362 (2007).
12. B. Argunhan, Y. Murayama, H. Iwasaki, The differentiated and conserved roles of Swi5-Sfr1 in homologous recombination. *FEBS Lett.* **591**, 2035–2047 (2017).
13. C. Ellermeier, H. Schmidt, G. R. Smith, Swi5 acts in meiotic DNA joint molecule formation in Schizosaccharomyces pombe. *Genetics* **168**, 1891–1898 (2004).
14. N. Haruta, *et al.*, The Swi5-Sfr1 complex stimulates Rhp51/Rad51 - and Dmc1-mediated DNA strand exchange in vitro. *Nat. Struct. Mol. Biol.* **13**, 823–830 (2006).
15. Y. Murayama, Y. Kurokawa, Y. Tsutsui, H. Iwasaki, Dual regulation of Dmc1-driven DNA strand exchange by Swi5- Sfr1 activation and Rad22 inhibition. *Genes Dev.* **27**, 2299–2304 (2013).
16. R. W. Hyppa, G. R. Smith, Crossover Invariance Determined by Partner Choice for Meiotic DNA Break Repair. *Cell* **142**, 243–255 (2010).
17. A. Lorenz, *et al.*, The Fission Yeast FANCM Ortholog Directs Non-Crossover Recombination During Meiosis. *Science (80-.).* **336**, 1585–1588 (2012).
18. Y. Akamatsu, M. Jasin, Role for the mammalian Swi5-Sfr1 complex in DNA strand break repair through homologous recombination. *PLoS Genet.* **6**, 1–11 (2010).
19. A. Hayase, *et al.*, A protein complex containing Mei5 and Sae3 promotes the assembly of the meiosis-specific RecA homolog Dmc1. *Cell* **119**, 927–940 (2004).

20. H. Tsubouchi, G. S. Roeder, The budding yeast Mei5 and Sae3 proteins act together with Dmc1 during meiotic recombination. *Genetics* **168**, 1219–1230 (2004).
21. S. R. Ferrari, J. Grubb, D. K. Bishop, The Mei5-Sae3 protein complex mediates Dmc1 activity in Saccharomyces cerevisiae. *J. Biol. Chem.* **284**, 11766–11770 (2009).
22. K. Ito, Y. Murayama, M. Takahashi, H. Iwasaki, Two three-strand intermediates are processed during Rad51-driven DNA strand exchange. *Nat. Struct. Mol. Biol.* **25**, 29–36 (2018).
23. Y. Kurokawa, Y. Murayama, N. Haruta-Takahashi, I. Urabe, H. Iwasaki, Reconstitution of DNA strand exchange mediated by Rhp51 recombinase and two mediators. *PLoS Biol.* **6**, 836–848 (2008).
24. C. H. Lu, *et al.*, Swi5-Sfr1 stimulates Rad51 recombinase filament assembly by modulating Rad51 dissociation. *Proc. Natl. Acad. Sci. U. S. A.* **115**, E10059–E10068 (2018).
25. J. L. Gerton, J. L. DeRisi, Mnd1p: An evolutionarily conserved protein required for meiotic recombination. *Proc. Natl. Acad. Sci.* **99**, 6895–6900 (2002).
26. J.-Y. Leu, P. R. Chua, G. S. Roeder, The meiosis-specific Hop2 protein of S. cerevisiae ensures synapsis between homologous chromosomes. *Cell* **94**, 375–386 (1998).
27. K. Nabeshima, Y. Kakihara, Y. Hiraoka, H. Nojima, A novel meiosis-specific protein of fission yeast, Meu13p, promotes homologous pairing independently of homologous recombination. *EMBO J.* **20**, 3871–3881 (2001).
28. T. T. Saito, T. Tougan, T. Kasama, D. Okuzaki, H. Nojima, Mcp7, a meiosis-specific coiled-coil protein of fission yeast, associates with Meu13 and

is required for meiotic recombination. *Nucleic Acids Res.* **32**, 3325–3339 (2004).

29. H. Tsubouchi, G. S. Roeder, The Mnd1 Protein Forms a Complex with Hop2 To Promote Homologous Chromosome Pairing and Meiotic Double-Strand Break Repair. *Mol. Cell. Biol.* **22**, 3078–3088 (2002).
30. C. Zierhut, M. Berlinger, C. Rupp, A. Shinohara, F. Klein, Mnd1 is required for meiotic interhomolog repair. *Curr. Biol.* **14**, 752–762 (2004).
31. J. B. Crickard, Y. Kwon, P. Sung, E. C. Greene, Dynamic interactions of the homologous pairing 2 (Hop2)–meiotic nuclear divisions 1 (Mnd1) protein complex with meiotic presynaptic filaments in budding yeast. *J. Biol. Chem.* **294**, 490–501 (2019).
32. Y. L. Chan, M. S. Brown, D. Qin, N. Handa, D. K. Bishop, The third exon of the budding yeast meiotic recombination gene HOP2 is required for calcium-dependent and recombinase Dmc1-specific stimulation of homologous strand assimilation. *J. Biol. Chem.* **289**, 18076–18086 (2014).
33. Y.-K. Chen, *et al.*, Heterodimeric complexes of Hop2 and Mnd1 function with Dmc1 to promote meiotic homolog juxtaposition and strand assimilation. *Proc. Natl. Acad. Sci.* **101**, 10572–10577 (2004).
34. M. Ploquin, *et al.*, Stimulation of fission yeast and mouse Hop2-Mnd1 of the Dmc1 and Rad51 recombinases. *Nucleic Acids Res.* **35**, 2719–2733 (2007).
35. H. Tsubouchi, G. S. Roeder, The importance of genetic recombination for fidelity of chromosome pairing in meiosis. *Dev. Cell* **5**, 915–925 (2003).
36. C. Uanschou, *et al.*, Sufficient Amounts of Functional HOP2/MND1 Complex Promote Interhomolog DNA Repair but Are Dispensable for Intersister DNA Repair during Meiosis in Arabidopsis . *Plant Cell* **25**, 4924–4940 (2013).

37. P. Chi, J. San Filippo, M. G. Sehorn, G. V. Petukhova, P. Sung, Bipartite stimulatory action of the Hop2-Mnd1 complex on the Rad51 recombinase. *Genes Dev.* **21**, 1747–1757 (2007).

38. R. Enomoto, *et al.*, Stimulation of DNA strand exchange by the human TBPIP/Hop2-Mnd1 complex. *J. Biol. Chem.* **281**, 5575–5581 (2006).

39. G. V. Petukhova, *et al.*, The Hop2 and Mnd1 proteins act in concert with Rad51 and Dmc1 in meiotic recombination. *Nat. Struct. Mol. Biol.* **12**, 449–453 (2005).

40. R. J. Pezza, O. N. Voloshin, F. Vanevski, R. D. Camerini-Otero, Hop2/Mnd1 acts on two critical steps in Dmc1-promoted homologous pairing. *Genes Dev.* **21**, 1758–1766 (2007).

41. R. J. Pezza, *et al.*, The dual role of HOP2 in mammalian meiotic homologous recombination. *Nucleic Acids Res.* **42**, 2346–2357 (2014).

42. A. Piazza, W. D. Wright, W. D. Heyer, Multi-invasions Are Recombination Byproducts that Induce Chromosomal Rearrangements. *Cell* **170**, 760-773.e15 (2017).

43. R. J. Pezza, R. D. Camerini-Otero, P. R. Bianco, Hop2-Mnd1 condenses DNA to stimulate the synapsis phase of DNA strand exchange. *Biophys. J.* **99**, 3763–3772 (2010).

44. W. Zhao, *et al.*, Mechanistic insights into the role of Hop2-Mnd1 in meiotic homologous DNA pairing. *Nucleic Acids Res.* **42**, 906–917 (2014).

45. P. Sung, L. Krejci, S. Van Komen, M. G. Sehorn, Rad51 Recombinase and Recombination Mediators. *J. Biol. Chem.* **278**, 42729–42732 (2003).

46. H. A. Kang, *et al.*, Crystal structure of Hop2-Mnd1 and mechanistic insights into its role in meiotic recombination. *Nucleic Acids Res.* **43**, 3841–3856 (2015).

47. R. J. Pezza, G. V. Petukhova, R. Ghirlando, R. D. Camerini-Otero, Molecular activities of meiosis-specific proteins Hop2, Mnd1, and the Hop2-Mnd1 complex. *J. Biol. Chem.* **281**, 18426–18434 (2006).

48. A. F. Say, *et al.*, The budding yeast Mei5–Sae3 complex interacts with Rad51 and preferentially binds a DNA fork structure. *DNA Repair (Amst).* **10**, 586–594 (2011).

49. N. Kuwabara, *et al.*, Mechanistic insights into the activation of Rad51-mediated strand exchange from the structure of a recombination activator, the Swi5-Sfr1 complex. *Structure* **20**, 440–449 (2012).

50. Y. L. Chan, A. Zhang, B. P. Weissman, D. K. Bishop, RPA resolves conflicting activities of accessory proteins during reconstitution of Dmc1-mediated meiotic recombination. *Nucleic Acids Res.* **47**, 747–761 (2019).

51. V. Cloud, Y.-L. Chan, J. Grubb, B. Budke, D. K. Bishop, Rad51 Is an Accessory Factor for Dmc1-Mediated Joint Molecule Formation During Meiosis. *Science (80-.).* **337**, 1222–1225 (2012).

52. W. Zhao, P. Sung, Significance of ligand interactions involving Hop2-Mnd1 and the RAD51 and DMC1 recombinases in homologous DNA repair and XX ovarian dysgenesis. *Nucleic Acids Res.* **43**, 4055–4066 (2015).

53. D. V. Bugreev, *et al.*, HOP2-MND1 modulates RAD51 binding to nucleotides and DNA. *Nat. Commun.* **5**, 1–10 (2014).

54. P. Chi, *et al.*, Yeast recombination factor Rdh54 functionally interacts with the Rad51 recombinase and catalyzes Rad51 removal from DNA. *J. Biol. Chem.* **281**, 26268–26279 (2006).

55. P. Chi, *et al.*, Functional interactions of meiotic recombination factors Rdh54 and Dmc1. *DNA Repair (Amst).* **8**, 279–284 (2009).

56. W. D. Wright, W. D. Heyer, Rad54 Functions as a Heteroduplex DNA Pump Modulated by Its DNA Substrates and Rad51 during D Loop Formation. *Mol. Cell* **53**, 420–432 (2014).

57. M. G. Catlett, S. L. Forsburg, Schizosaccharomyces pombe Rdh54 (TID1) Acts with Rhp54 (RAD54) to Repair Meiotic Double-Strand Breaks. *Mol. Biol. Cell* **14**, 4707–4720 (2003).

58. C. Kerzendorfer, The Arabidopsis thaliana MND1 homologue plays a key role in meiotic homologous pairing, synapsis and recombination. *J. Cell Sci.* **119**, 2486–2496 (2006).

59. G. V. Petukhova, P. J. Romanienko, R. D. Camerini-Otero, The Hop2 protein has a direct role in promoting interhomolog interactions during mouse meiosis. *Dev. Cell* **5**, 927–936 (2003).

60. J. Vignard, *et al.*, The interplay of RecA-related proteins and the MND1-HOP2 complex during meiosis in Arabidopsis thaliana. *PLoS Genet.* **3**, 1894–1906 (2007).

61. M. A. Ramesh, S.-B. Malik, J. M. Logsdon, A Phylogenomic Inventory of Meiotic Genes. *Curr. Biol.* **15**, 185–191 (2005).

62. S. Domenichini, C. Raynaud, D. A. Ni, Y. Henry, C. Bergounioux, Atmnd1-Δ1 is sensitive to gamma-irradiation and defective in meiotic DNA repair. *DNA Repair (Amst).* **5**, 455–464 (2006).

63. L. Ko, G. R. Cardona, A. Henrion-Caude, W. W. Chin, Identification and Characterization of a Tissue-Specific Coactivator, GT198, That Interacts with the DNA-Binding Domains of Nuclear Receptors. *Mol. Cell. Biol.* **22**, 357–369 (2002).

64. N. W. Cho, R. L. Dilley, M. A. Lampson, R. A. Greenberg, Interchromosomal homology searches drive directional ALT telomere movement and synapsis. *Cell* **159**, 108–121 (2014).

65. J. Schindelin, *et al.*, Fiji: an open-source platform for biological-image analysis. *Nat. Methods* **9**, 676 (2012).

Figure Legends

Fig. 1. Hop2-Mnd1 stimulates Dmc1-mediated strand exchange, leading to robust accumulation of hyper JMs.

(A) Schematic of the in vitro strand exchange assay using PhiX174 DNA as substrates.

(B) Circular single-stranded DNA (css) was first incubated with Dmc1, then mixed with Hop2-Mnd1, RPA, and finally with linear double-stranded DNA (lds), followed by a further incubation for 2 h at 30˚C. The products were analyzed by agarose gel electrophoresis. The signal denoted with asterisks corresponds to “hyper JMs”, which are defined as JMs bigger than those normally formed in reactions containing Swi5-Sfr1.

(C) Time course analysis of Dmc1-mediated strand exchange promoted by either Hop2-Mnd1 or Swi5-Sfr1.

(D) Synergistic activation of Dmc1 by Hop2-Mnd1 and Swi5-Sfr1. Dmc1 was preincubated with ssDNA, then mixed with the indicated auxiliary factor(s) and the reaction was incubated for 1 h at 30˚C. In **(B-D)**, the following concentrations of substrates were used: Dmc1, 5 μM; RPA, 1 μM; css, 10 μM; lds, 10 μM. In **(C, D)**, Swi5-Sfr1 and Hop2-Mnd1 were used at concentrations of 0.5 μM and 0.25 μM, respectively. css, circular ssDNA; lds, linear dsDNA; JM, joint molecules; nc, nicked circular DNA**.**

For the graphs in **(B-D)**, mean values ± SD from three independent experiments are shown.

Fig. 2. Hop2-Mnd1 stimulates efficient strand exchange by bypassing the donor dsDNA end-dependency.

(A) dsDNA ends examined in the strand exchange reactions in **(B)**.

(B) Strand exchange reactions were conducted with linear dsDNA with various ends as indicated. Circular single-stranded DNA (css) was first incubated with Dmc1 for 5 min, then supplemented with Swi5-Sfr1 or Hop2-Mnd1 and RPA, and incubated for a further 5 min. The reaction was then initiated through the addition of linear double-stranded DNA (lds) and incubated for 1 h at 30˚C. Reaction products were analyzed by agarose gel electrophoresis. Dmc1, 5 μM; Swi5-Sfr1, 0.5 μM; Hop2-Mnd1, 0.25 μM; RPA, 1 μM; css, 10 μM; lds, 10 μM. css, circular ssDNA; lds, linear dsDNA; JM, joint molecules; nc, nicked circular DNA**.** Mean values ± SD from three independent experiments are shown.

Fig. 3. Hop2-Mnd1 is not an efficient stabilizer of the Dmc1 presynaptic filament.

(A) Dmc1-driven strand exchange reaction with RPA-precoated ssDNA. ssDNA (css) was precoated with RPA, then mixed with Dmc1, dsDNA and the indicated auxiliary factor.

(B) Schematic of the RPA chase assay.

(C) RPA chase assay. css annealed to biotinylated oligos was initially precoated with Dmc1, then incubated in the presence of the indicated auxiliary factor, followed by the addition of RPA. css was precipitated with streptavidin-coated magnetic beads and associated proteins were examined (css-bound), along with proteins left in the supernatant (unbound), by SDS-PAGE. Dmc1, 5 μM; Hop2-Mnd1, 0.25 or 0.5 μM; Swi5-Sfr1, 0.5 or 1 μM; RPA, 1 μM; css, 10 μM.

(D) Presynaptic filament stability assayed by fluorescence anisotropy. Dmc1 presynaptic filaments were formed by mixing Dmc1 with fluorescently labelled oligo-dT (72-mer), then the mixture was incubated with the indicated auxiliary factor. Stability of the formed filaments was examined by diluting the mixture (40-fold) and monitoring the change in fluorescence anisotropy over time.

(E) Synergistic activation of Dmc1-driven strand exchange by Hop2-Mnd1 and Swi5-Sfr1 with RPA-precoated ssDNA. ssDNA precoated with RPA was mixed with Dmc1, the indicated auxiliary factor(s) and linear dsDNA prepared with StuI. The reaction was then incubated at 30˚C for 60 min. Dmc1, 5 μM; Swi5-Sfr1, 4 μM; Hop2-Mnd1, 1 μM; RPA, 2 μM; css, 10 μM; lds, 10 μM. css, circular ssDNA; lds, linear dsDNA; JM, joint molecules; nc, nicked circular DNA**.**

For the graphs in **(A,C,E)**, mean values ± SD from three independent experiments are shown. Representative kinetics of the reactions are shown in **(D)**.

Fig. 4. Hop2-Mnd1 allows Dmc1 to exchange strands with homology embedded within nonhomologous DNA.

(A) Schematic of the D-loop assay employing a linear ssDNA and either linear dsDNA (left) or nicked circular DNA (right).

(B) Gel images of the D-loop assay with naked linear ssDNA (lss).

(C) Gel images of the D-loop assay with RPA-precoated linear ssDNA (lss).

In **(B**,**C),** linear dsDNA (lds, left) or nicked circular DNA (nc, right) was used. In **(B)**, lss was preincubated with Dmc1, then mixed with auxiliary factor(s) and dsDNA. In **(C)**, lss was precoated with RPA, then mixed with Dmc1, auxiliary factor(s) and dsDNA. After addition of dsDNA, the reaction was incubated at 30˚C for 1 h. Yield is expressed as the percentage of the signal for the products to the sum of the products and either lds or nc. Dmc1, 5 μM; Swi5-Sfr1, 0.5 μM in **(B)** and 4 μM in **(C)**; Hop2-Mnd1, 0.25 μM; RPA, 1 μM; lss, 5 μM; lds, 5 μM; nc, 5 μM. For the graphs in **(B,C)**, mean values ± SD from three independent experiments are shown.

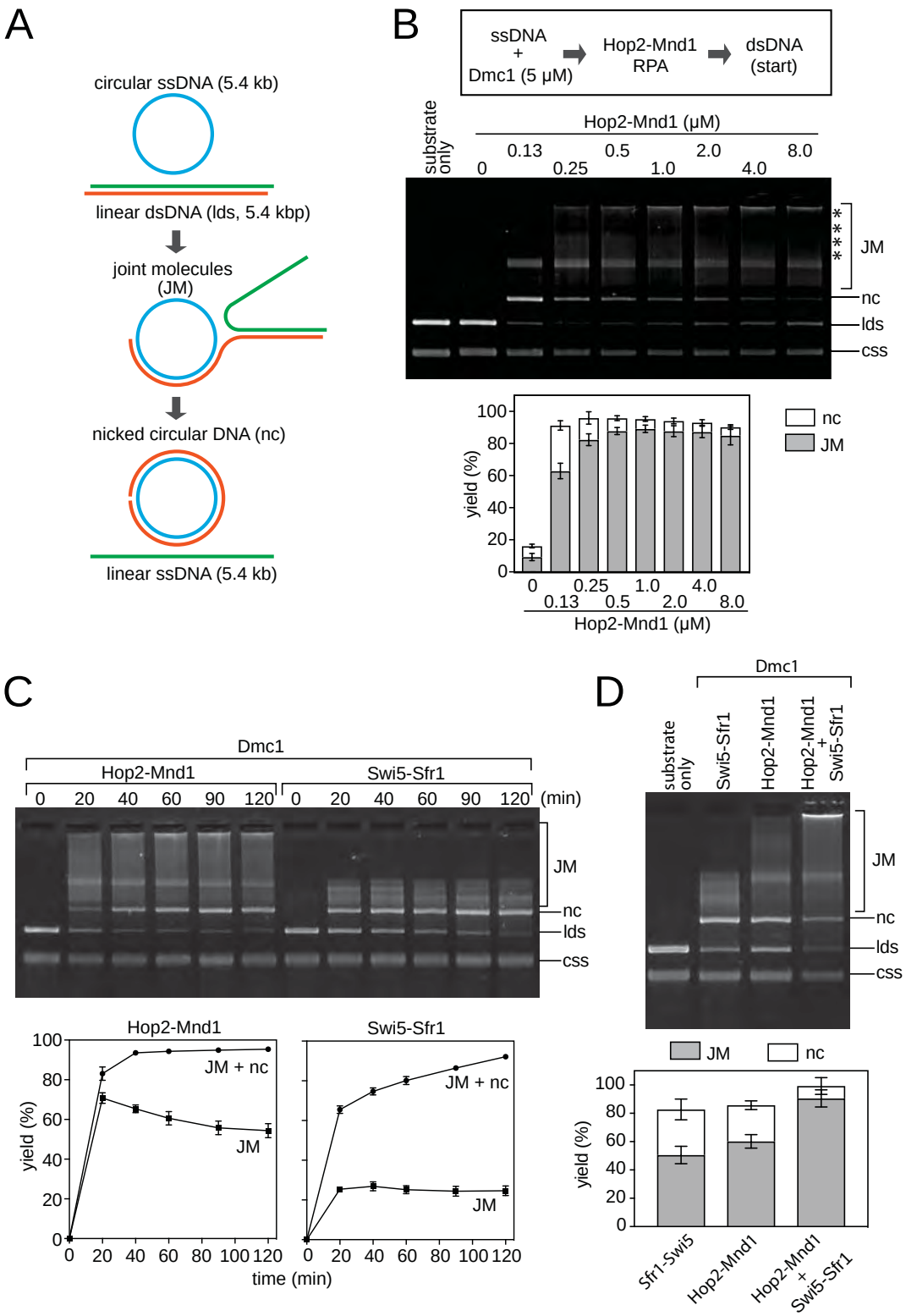
Fig. 5. The effect of heterology at linear ssDNA ends on strand exchange.

(A) Schematic of the D-loop assay using linear ssDNA with heterology (70 bp) at its end(s).

(B) Linear ssDNA (lss) was preincubated with Dmc1, then mixed with auxiliary factor(s), RPA and linear dsDNA (lds). The reaction was then incubated at 30˚C for 1 h. Dmc1, 5 μM; Swi5-Sfr1, 0.5 μM; Hop2-Mnd1, 0.25 μM; RPA, 1 μM; lss, 5 μM; lds, 5 μM.

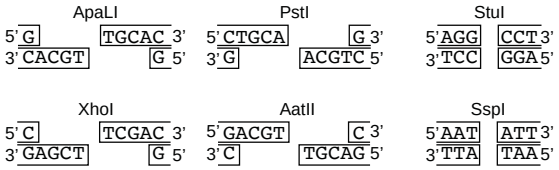
(C) Quantification of results shown in **(B)**. Yield is expressed as the percentage of the signal for the products to the sum of the lds and products. Mean values ± SD from three independent experiments are shown.

(D) Stepwise involvement of two auxiliary factors in the establishment of Dmc1-driven synapsis. **[a.]** Following meiotic DSB formation and end-resection, RPA binds to the ssDNA exposed at a DSB end. **[b.]** Swi5-Sfr1 functions as a canonical “mediator” and facilitates the replacement of RPA with Dmc1, which forms a nucleoprotein filament. **[c.]** Hop2-Mnd1 executes its role as an initiator of strand exchange by allowing the Dmc1 filament to invade a donor dsDNA duplex, which constitutes initiation of the synaptic phase. **[d.]** Swi5-Sfr1 and Hop2-Mnd1 may then promote further strand transfer within the synaptic phase, leading to heteroduplex extension. See text for more details.

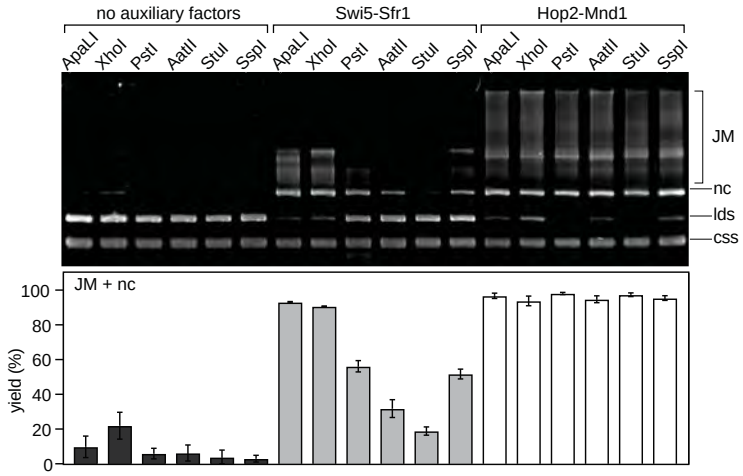

A
circular ssDNA (5.4 kb)
linear dsDNA (lds, 5.4 kbp)
joint molecules (JM)
nicked circular DNA (nc)
linear ssDNA (5.4 kb)
B
ssDNA + Dmc1 (5 μM)
Hop2-Mnd1 RPA
dsDNA (start)
substrate only
Hop2-Mnd1 (μM)
0
0.13
0.25
0.5
1.0
2.0
4.0
8.0
JM
nc
lds
css
yield (%)
nc
JM
C
Dmc1
Hop2-Mnd1
Swi5-Sfr1
0 20 40 60 90 120 0 20 40 60 90 120 (min)
JM
nc
lds
css
Hop2-Mnd1
Swi5-Sfr1
JM + nc
JM
yield (%)
time (min)
D
Dmc1
substrate only
Swi5-Sfr1
Hop2-Mnd1
Hop2-Mnd1 + Swi5-Sfr1
JM
nc
lds
css
JM
nc
yield (%)
Sfr1-Swi5
Hop2-Mnd1
Hop2-Mnd1 + Swi5-Sfr1

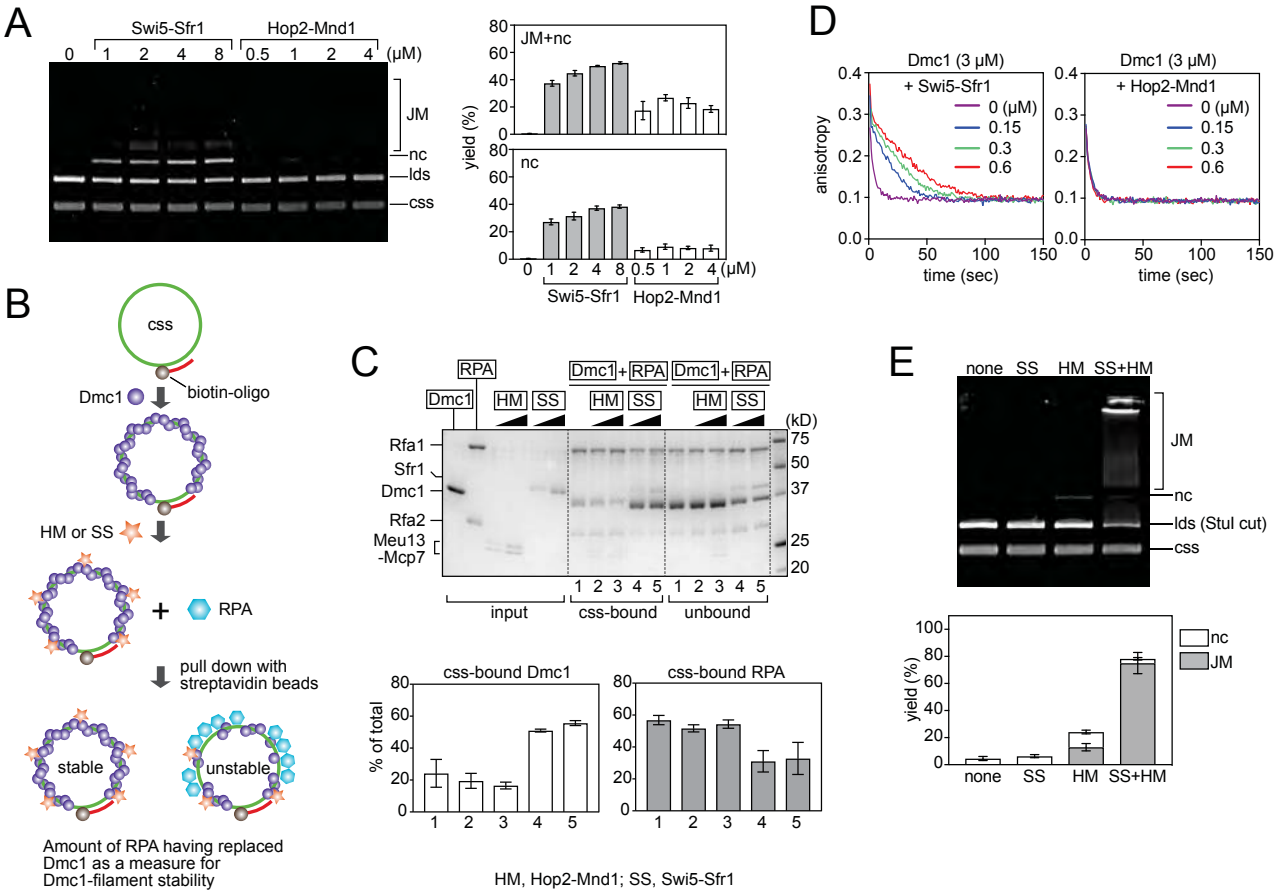
Tsubouchi_Fig2

A

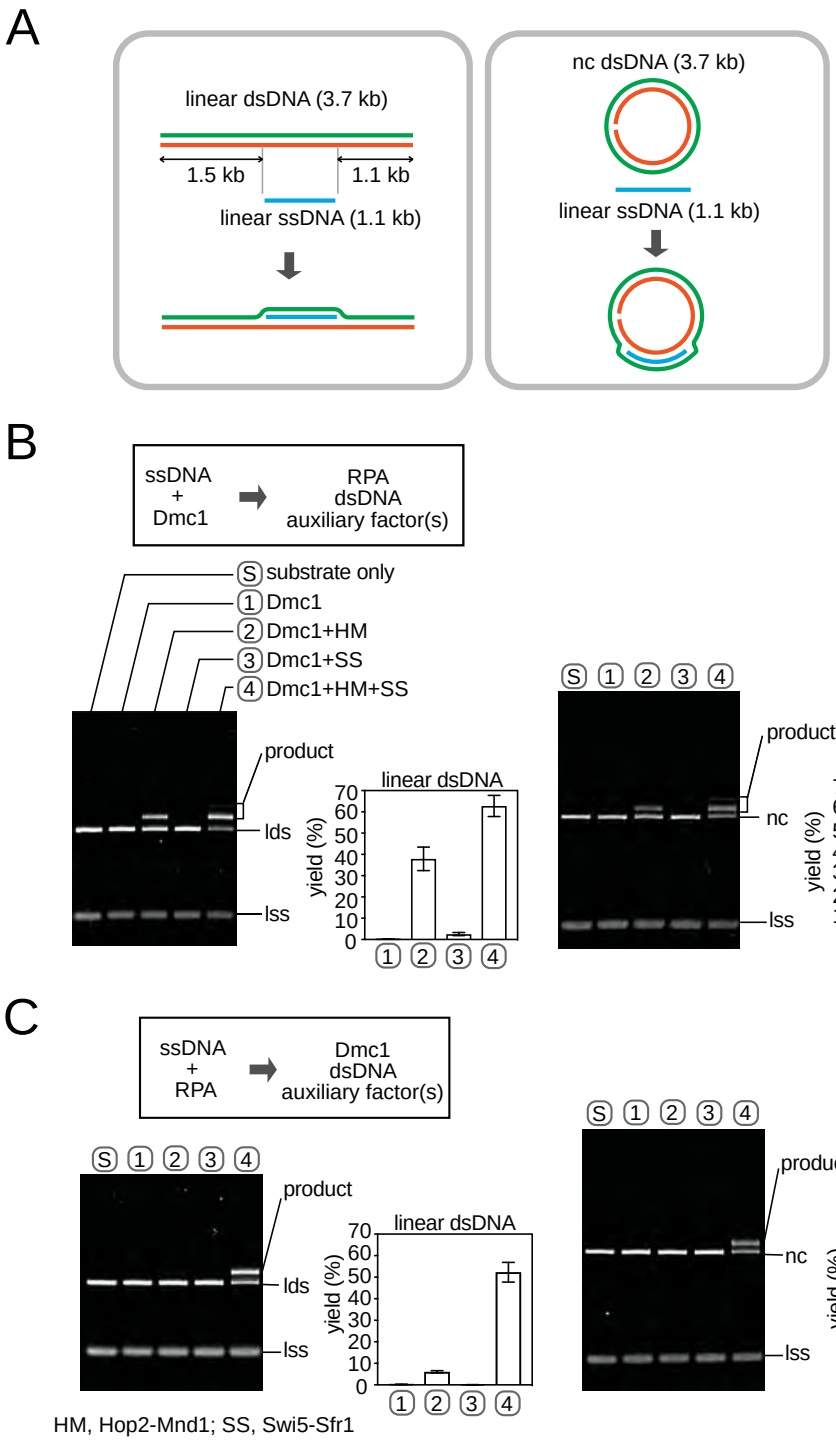


B

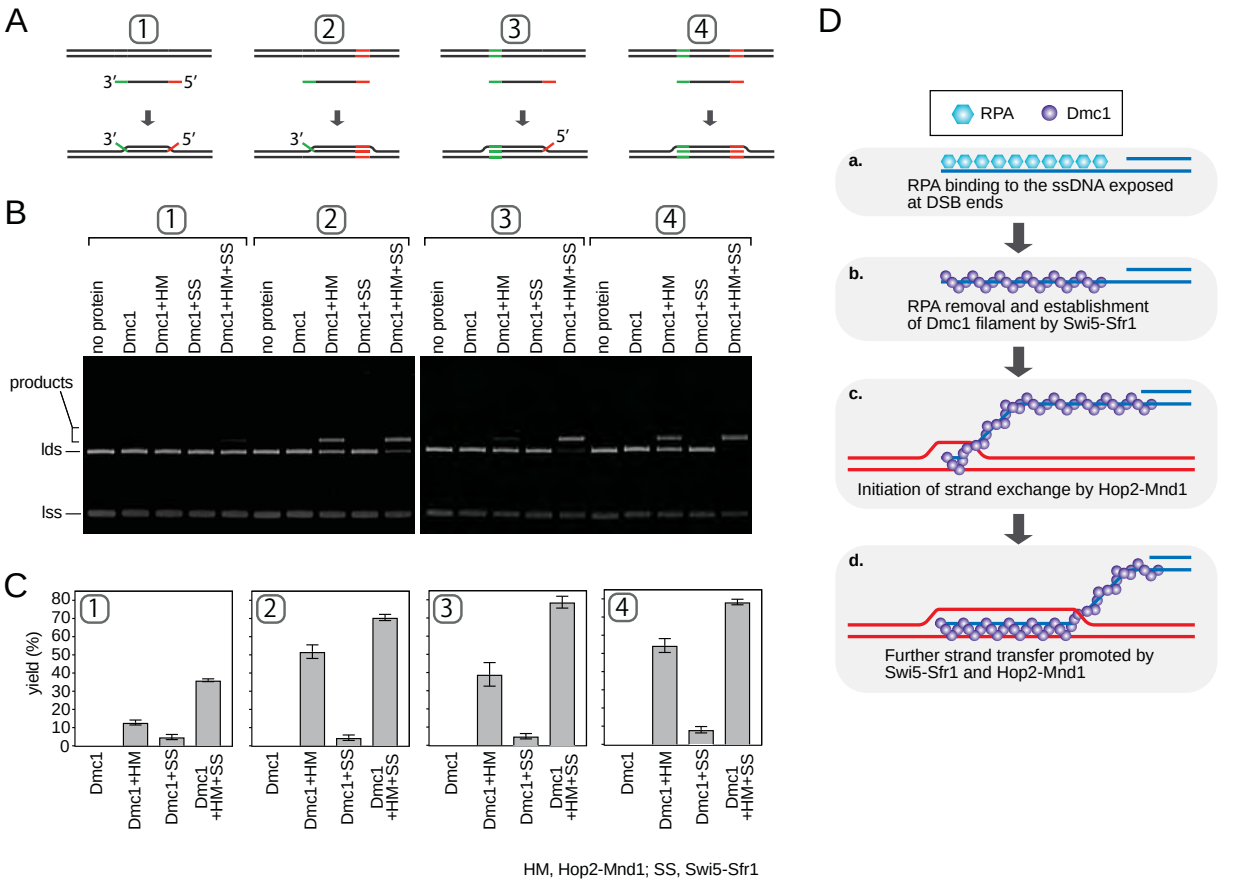



A
Swi5-Sfr1
Hop2-Mnd1
0 1 2 4 8 0.5 1 2 4 (μM)
JM
nc
lds
css
JM+nc
nc
yield (%)
0 1 2 4 8 0.5 1 2 4 (μM)
Swi5-Sfr1
Hop2-Mnd1
B
css
Dmc1
biotin-oligo
HM or SS
RPA
pull down with
streptavidin beads
stable
unstable
Amount of RPA having replaced
Dmc1 as a measure for
Dmc1-filament stability
C
RPA
Dmc1
Dmc1+RPA
HM
SS
(kD)
Rfa1
Sfr1
Dmc1
Rfa2
Meu13
-Mcp7
75
50
37
25
20
1 2 3 4 5 1 2 3 4 5
input
css-bound
unbound
css-bound Dmc1
% of total
css-bound RPA
HM, Hop2-Mnd1; SS, Swi5-Sfr1
D
Dmc1 (3 μM)
+ Swi5-Sfr1
0 (μM)
0.15
0.3
0.6
anisotropy
time (sec)
Dmc1 (3 μM)
+ Hop2-Mnd1
E
none SS HM SS+HM
JM
nc
lds (StuI cut)
css
yield (%)
nc
JM
none SS HM SS+HM

Tsubouchi_Fig4



Tsubouchi_Fig5



HM, Hop2-Mnd1; SS, Swi5-Sfr1

Supplementary Information for

Two Auxiliary Factors Promote Dmc1-Driven DNA Strand Exchange via Stepwise Mechanisms

Hideo Tsubouchi[1,3,*], Bilge Argunhan[1], Kentaro Ito[1], Masayuki Takahashi[2], Hiroshi Iwasaki[1,3]

***Lead contact: htsubouchi@bio.titech.ac.jp**

This PDF file includes:

Supplementary text

Figures S1 to S5

SI References

Supplementary Information Text

SI Materials and Methods

E. coli Strain and Media

For protein production conducted in this study, BL21-CodonPlus(DE3)-RIPL (Agilent technologies) was used. Standard media was used for growth (LB) and selection (LB with antibiotics).

Plasmids and DNA Substrates

pET15b-3C, in which the original thrombin cleavage site was replaced with the PreScission protease cleavage site, was used to clone the cDNA of Hop2 and Mnd1 (*S. pombe meu13*$^{+}$ and *mcp7*$^{+}$, obtained from National BioResource Project) so that the insert carries *HOP2*, a ribosomal binding site, and *MND1*, in this order.

yEGFP was amplified as two fragments by PCR using pTOW-PYK1 (1) with two pairs of primers (92-93 and 94-95), then cloned in the SmaI site of pBluescriptII KS, with a new Nb.BbvCI site created within yEGFP. The mutated yEGFP was amplified using primers 95-135 to create an Nt.BspQI site right before the start codon of yEGFP, yielding plasmid p101. An Nb.BsmI site was introduced into p101 by PCR using p101 and primers 206-207 to create p159, which was used as a nicked circular dsDNA substrate after digestion with Nb.BsmI (NEB). Two different 70-bp sequences (both from the *S. cerevisiae URA3* gene) were introduced either before the start codon or after the stop codon, by using primer pairs 208-211 and 209-210, to create p160 and p161, respectively. For introduction of insertions at

both ends, primer pair 210-211, and a fragment amplified with p159 (template) and primers 208 and 209 were used to create p162. p101 and p162 were digested by Nt.BspQI (NEB), releasing the 1070 nt ssDNA, which was gel-purified after denaturing at 80°C for 5 min in the presence of 8.3 mM Tris-HCl (8.0), 6.7 M urea, 0.83% igepal CA-630 and used as a linear ssDNA substrate. p159, 160, 161 and 162 were digested by ScaI (NEB) to create linear dsDNA substrates. All the DNA substrates were gel purified using MonoFas DNA purification kit I (GL Sciences Inc.), and concentrations are expressed in μM nucleotide (μMnt).

Protein Purification for Biochemical Analyses

All the proteins used in this study were produced using BL21-CodonPlus(DE3)-RIPL. Purification of Dmc1, Rad51, RPA, and Swi5-Sfr1 were described previously (2–4). Protein purification was conducted at 4°C. Purified proteins were checked for nuclease contamination, which was below detectable levels in the assay conditions employed here.

Rad51 was expressed from plasmid pET11b with 1 mM IPTG at 18°C for 12 h. Harvested cells were lysed by sonication, cleared (70,000 *g*, 1 h) and precipitated with ammonium sulfate to 35% saturation. The protein mixture was centrifuged (10,000 *g*, 30 min) and the pellet was resuspended in P buffer (20 mM potassium phosphate [pH 7.4], 0.5 mM EDTA, 10% glycerol, 1 mM DTT). The protein solution was applied to SP Sepharose (GE Healthcare), and the flow-through fraction was then applied to Q Sepharose (GE Healthcare) and eluted with a gradient from 100 mM to 800 mM KCl. Combined peak fractions were applied to HiTrap Heparin, then eluted with a gradient from 100 mM to 700 mM KCl. The combined peak fractions

were then applied to Resource Q (GE Healthcare) and eluted with a gradient from 100 mM to 600 mM KCl. Peak fractions were pooled, dialyzed against P buffer containing 200mM KCl, concentrated in Amicon Ultra-4 (MWCO 10,000), frozen in liquid nitrogen and stored at -80°C.

Dmc1 was expressed from plasmid pET28a and the same conditions as Rad51 were employed for cell lysis and lysate clearing. Ammonium sulfate precipitation was with 60% saturation. The protein mixture was centrifuged (10,000 *g*, 30 min) and the pellet was resuspended in R buffer (20 mM Tris-HCl [pH 8.0], 1 mM EDTA, 10% glycerol, 1 mM DTT). The protein solution was applied to SP Sepharose (GE Healthcare), and the flow-through was then applied to Q Sepharose (GE Healthcare) and eluted with a gradient from 100 mM to 800 mM KCl. Combined peak fractions were applied to HiTrap Heparin, then eluted with a gradient from 100 mM to 800 mM KCl. Combined peak fractions were then developed in a Superdex 200 PG 16/60 column in R buffer containing 0.5 M NaCl. The combined peak fractions were then applied to Resource Q and eluted with a gradient from 100 mM to 600 mM KCl. Peak fractions were pooled, dialyzed against R buffer containing 200 mM KCl, concentrated in Amicon Ultra-4 (MWCO 10,000), frozen in liquid nitrogen and stored at -80°C.

For RPA purification, Ssb1, Ssb2 and Ssb3 (fission yeast counterparts of Rfa1, Rfa2 and Rfa3, respectively) were co-expressed with intervening ribosome binding sites from pET11b. The same conditions as Rad51 were employed for protein expression and lysate clearing. Polyethyleneimine was added to the cleared lysate to a final concentration of 0.05% and the protein mixture was centrifuged (20,000 *g*, 30 min). The supernatant was fractionated by ammonium sulfate

precipitation (40% saturation). The pellet was resuspended in R buffer containing 1 M NaCl then dialyzed against R buffer with 100 mM NaCl. The sample was applied to SP Sepharose and eluted with a gradient from 100 mM to 1 M NaCl. Combined peak fractions were then applied to HiTrap Heparin and eluted with a gradient from 100mM to 700mM NaCl. Combined peak fractions was then developed in a Superdex 200 PG 16/60 column in R buffer containing 1 M NaCl. Peak fractions were pooled, dialyzed against R buffer ~~at~~ containing 100 mM NaCl, then concentrated using Amicon Ultra-4 (MWCO 10,000), frozen in liquid nitrogen and at -80°C.

Sfr1 and Swi5 were co-expressed from plasmids pET28a and pET11b, respectively. The expression conditions, lysate clearing (polyethyleneimine and ammonium sulfate precipitation) and SP Sepharose fractionation were the same as for RPA except that ammonium sulfate precipitation was with 35% saturation and SP Sepharose fractionation was from 100 mM to 800 mM. Combined peak fractions was applied to HiTrap Heparin and eluted with a gradient from 100 mM to 800 mM NaCl. Combined peak fractions was then developed in a Superdex 200 PG 16/60 column in R buffer containing 1 M NaCl. Peak fractions were pooled, dialyzed against R buffer containing 200 mM NaCl, concentrated in Amicon Ultra-4 (MWCO 10,000) and stored at -80°C. Swi5-Sfr1 was purified as a stable heterodimer throughout the purification as reported previously (5).

Hop2 and Mnd1 were co-expressed with an intervening ribosome binding site from pET11b. The same conditions as Dmc1 were employed for protein expression and lysate clearing. The protein solution was incubated with Nickel-conjugated resin (Roche) for 1.5 h, washed with R buffer containing 200 mM KCl and 10 mM

imidazole, followed by elution with R buffer containing 200 mM KCl and 200 mM imidazole. The eluate was dialyzed against R buffer with 200 mM KCl and, for preparing untagged Hop2-Mnd1, PreScission (GE Healthcare) protease was added. Then the sample was applied to HiTrap Heparin and eluted with a gradient from 100 mM to 800 mM KCl. Combined peak fractions was applied to Resource S (GE Healthcare), eluted with a gradient from 50 mM to 1 M KCl. Peak fractions were pooled, dialyzed against R buffer containing 200 mM KCl, concentrated in Amicon Ultra-4 (MWCO 10,000), frozen in liquid nitrogen and stored at -80°C. Hop2-Mnd2 was purified as a stable heterodimer throughout the purification. Tagged Hop2-Mnd1 was only used for protein-protein interaction assays.

In vitro Interaction Assay

Purified His6-Hop2-Mnd1, Dmc1, Rad51, Swi5-Sfr1 and RPA were used at 3 μM. Proteins alone or in combination with other proteins, as indicated, were mixed in the assay buffer (35 mM Tris-HCl [pH 7.5], 100 mM NaCl, 3.5 mM $MgCl_2$, 5% glycerol, 0.1% igepal CA-630, 20 mM imidazole). The protein mixture was incubated at 30°C for 15 min, followed by 4°C for 30 min, then mixed with Ni-magnetic beads (Dynabeads His-tag isolation and pulldown, Thermo Fisher Scientific). The mixture was further incubated at 4°C for 2 h with gentle agitation. Finally, a magnetic stand was used to separate the beads (precipitates, P) from the supernatant (S). Both fractions were denatured using Laemmli buffer and analyzed by SDS-PAGE and CBB staining.

RPA Chase Assay

Circular ssDNA (PhiX174 virion DNA, NEB) was conjugated to Dynabeads M-280 Streptavidin (Thermo Fisher Scientific) using a synthetic biotinylated oligonucleotide as described previously (3). RPA chase buffer (30 mM Tris-Cl [pH 7.5], 120 mM NaCl, 30 mM KCl, 3.5 mM $MgCl_2$, 2 mM ATP, 1 mM DTT, 5% glycerol) containing 10 μMnt css-beads was supplemented with 5 μM Dmc1 and incubated at 30°C with gentle agitation for 5 min. Either Hop2-Mnd1 (0.25 μM or 0.5 μM) or Swi5-Sfr1 (0.5 μM or 1 μM) was added and the reaction was further continued for 10 min at 30°C. Next, 1 μM RPA was added and the incubation was continued for 10 min at 30°C. Finally, a magnetic stand was used to separate the precipitate (css-bound) from the supernatant (unbound). Both fractions were denatured using Laemmli buffer and analyzed by SDS-PAGE. Following staining with Coomassie Brilliant Blue G-250, gels were imaged using a LAS4000 mini (GE Healthcare). Densitometric analysis was performed as described (3) except FIJI (6) was used instead. The values for RPA or Dmc1, in the supernatant (unbound) and precipitate (css-bound) fractions, were combined to obtain the sum. The yield is expressed as the percentage of the signal for css-bound divided by the sum. The values from three independent experiments were averaged and plotted along with error bars (SD).

dsDNA Capture Assay

css-conjugated magnetic beads, prepared as described above, were initially incubated with or without Dmc1 (5 μM) for 5 min at 30°C in the assay buffer (30 mM Tris-Cl [pH 7.5], 40 mM KCl, 3.5 mM $MgCl_2$, 2 mM AMP-PNP, 1 mM DTT, 100 ng/μL, BSA, 5% glycerol). The mixture of css-beads and Dmc1 was further incubated with or without Hop2-Mnd1 (1 μM) for 5 min at 30°C. The magnetic beads were

captured by the magnetic stand, and washed once with the assay buffer. The separated beads were then resuspended in the assay buffer and incubated with Ids (5 μMnt, either ApaLI-digested PhiX174 RF I or BamHI-digested pBluescript KS^+) at 30 °C for 30 min. Then the beads were captured again and the supernatant was collected. The beads were washed twice with assay buffer containing 0.01% Igepal and resuspend in assay buffer. Both the supernatant and the resuspended beads were treated with proteinase K (15 mg/mL) in the presence of 3% SDS at 30°C for 10 min. The supernatant of the bead-mixture was separated from the beads and used as the pellet fraction. Both the supernatant and the pellet fractions were analyzed by agarose gel electrophoresis. The signal values for the supernatant and the pellet were combined and set to 100% and the percentage of the pellet signal to the sum was presented as dsDNA pulldown efficiency. The values from three independent experiments were averaged and plotted with error bars (SD).

Dmc1 Nucleoprotein Filament Dissociation Assay

Anisotropy buffer (30 mM HEPES-KOH [pH 7.5], 120 mM KCl, 3 mM $MgCl_2$, 1 mM ATP, 1 mM DTT, 5% glycerol) containing 1.5 μMnt of oligo dT (72 mer) with a 5' TAMRA label was supplemented with 0.5 μM Dmc1 and incubated at 25 °C for 5 min. Next, either Swi5-Sfr1 or Hop2-Mnd1 was added at the indicated concentration and the reaction was continued for a further 5 min. This solution was transferred into a 0.3 x 0.3 cm quartz cuvette and the fluorescence anisotropy was monitored every second for 60 sec (25°C, excitation 546 nm, emission 575 nm) to confirm filament formation. Next, a 1.0 x 1.0 cm quartz cuvette containing 2 mL of anisotropy buffer was placed into the spectrofluorometer with constant stirring (450 rpm). After 60 sec

of measurement, 50 μL of the solution containing Dmc1 filaments with or without each auxiliary factor was injected into this cuvette. Fluorescence anisotropy was then monitored every second for 6 min. The data from three independent anisotropy experiments were averaged and plotted. Data were then regressed using KaleidaGraph with the exponential decay equation as follows: Anisotropy = (Amplitude of change in anisotropy) exp ($-k_{off}$ t) + (Minimum value of anisotropy), where k_{off} represents the dissociation rate constant and t represents time.

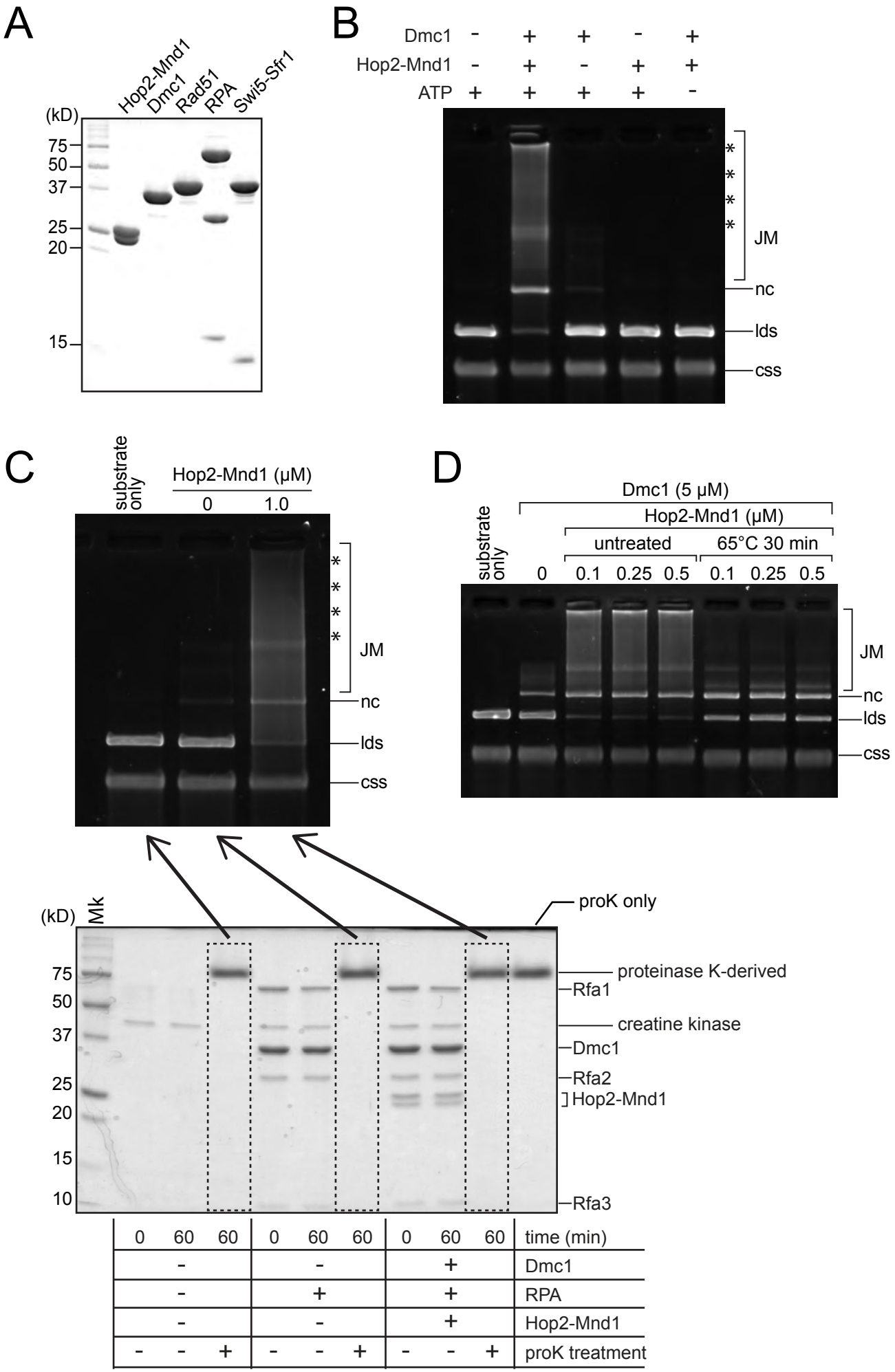

A
Hop2-Mnd1
Dmc1
Rad51
RPA
Swi5-Sfr1
(kD)
75
50
37
25
20
15
B
Dmc1 - + + - +
Hop2-Mnd1 - + - + +
ATP + + + + -
JM
nc
lds
css
C
substrate only
Hop2-Mnd1 (μM)
0
1.0
JM
nc
lds
css
D
Dmc1 (5 μM)
Hop2-Mnd1 (μM)
substrate only
untreated
65°C 30 min
0
0.1
0.25
0.5
0.1
0.25
0.5
JM
nc
lds
css
(kD)
Mk
75
50
37
25
20
15
10
proK only
proteinase K-derived
Rfa1
creatine kinase
Dmc1
Rfa2
Hop2-Mnd1
Rfa3
0 60 60 0 60 60 0 60 60 time (min)
- - + Dmc1
- + + RPA
- - + Hop2-Mnd1
- - + - - + - - + proK treatment

Fig. S1. Hyper JMs are produced by Dmc1.

(A) Proteins used in this study (4 μg loaded per lane).

(B) The three-strand exchange reaction was conducted with (+) or without (-) Dmc1 (5 μM), Hop2-Mnd1 (1 μM) and ATP (2 mM). Experiments were conducted as in Figure 1B, except that incubation time was 1 h.

(C) The three-strand exchange reaction was conducted as in Figure 1B, except that incubation time was 60 min and UV crosslinking was omitted. css was preincubated with Dmc1 (5 μM), followed by Hop2-Mnd1 (1 μM) and RPA (1 μM), then the reaction was initiated by adding lds. Samples were immediately withdrawn (0 min) and mixed with 2x SDS-PAGE loading buffer. Following 60 min of incubation, samples were withdrawn before and after proteinase K (proK) treatment, and mixed with 2x SDS-PAGE loading buffer. These samples were then analyzed by SDS-PAGE and CBB staining. The 60 min proK-treated reactions (denoted by dashed lines in the SDS-PAGE gel) were also subjected to agarose gel electrophoresis to detect strand-exchange products. The signal denoted with asterisks corresponds to “hyper JMs”.

(D) The products of the strand exchange reaction were incubated at 65˚C for 30 min then subjected to analysis.

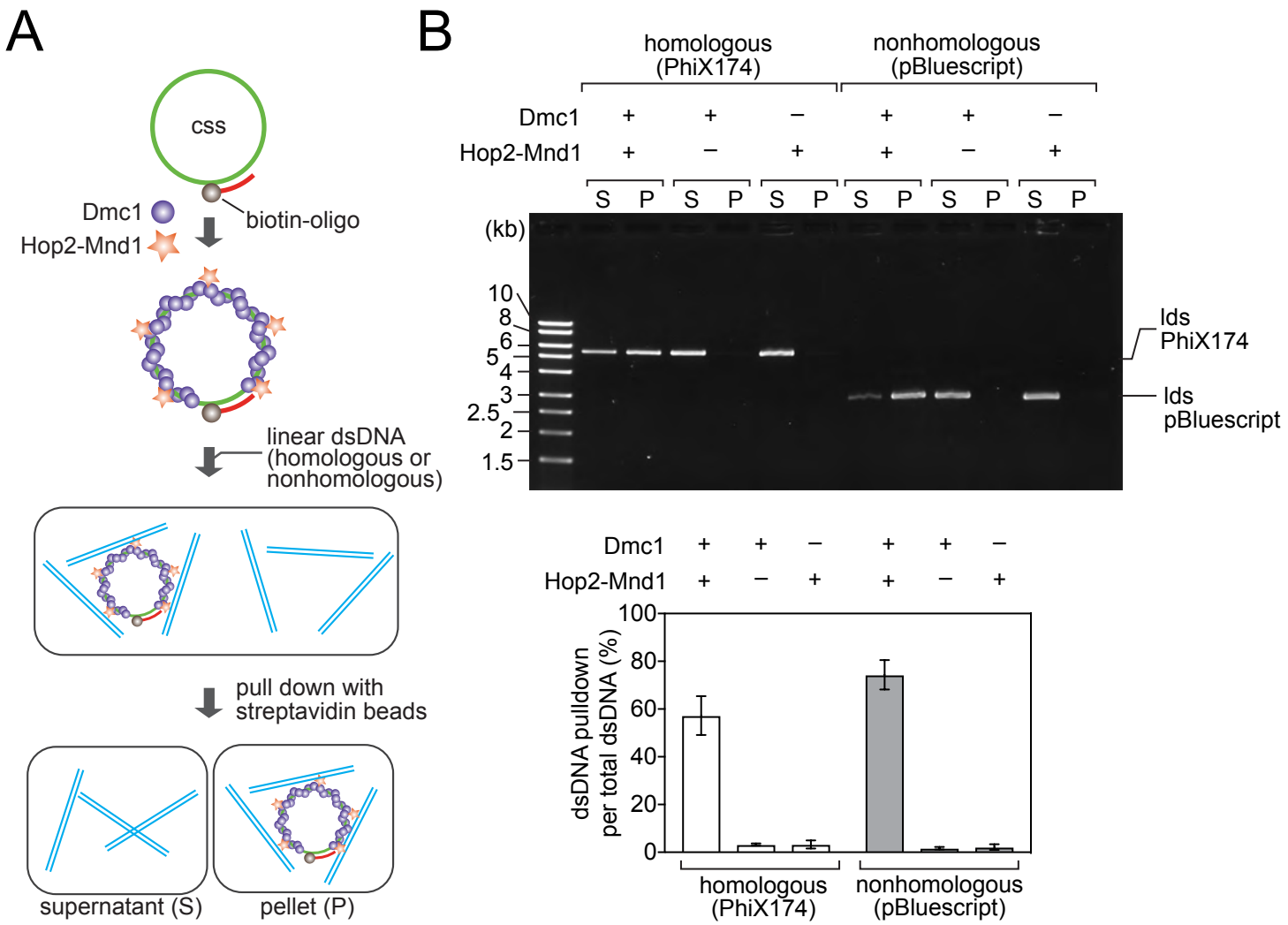
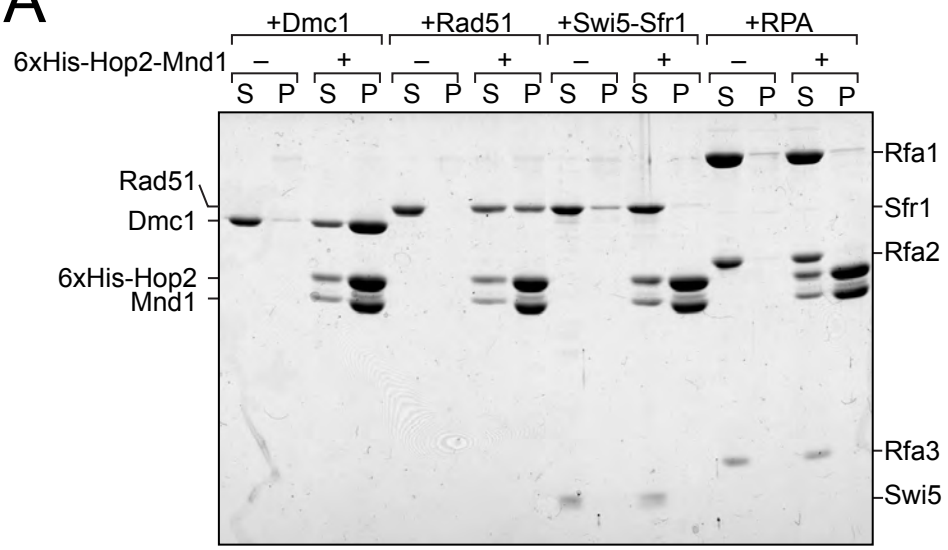

A
css
Dmc1
Hop2-Mnd1
biotin-oligo
linear dsDNA
(homologous or
nonhomologous)
pull down with
streptavidin beads
supernatant (S)
pellet (P)
B
homologous
(PhiX174)
nonhomologous
(pBluescript)
Dmc1
Hop2-Mnd1
S P S P S P S P S P S P
(kb)
10
8
6
5
4
3
2.5
2
1.5
lds
PhiX174
lds
pBluescript
dsDNA pulldown
per total dsDNA (%)
100
80
60
40
20
0
homologous
(PhiX174)
nonhomologous
(pBluescript)

Fig. S2. Hop2-Mnd1 facilitates dsDNA capture by Dmc1 presynaptic filaments.

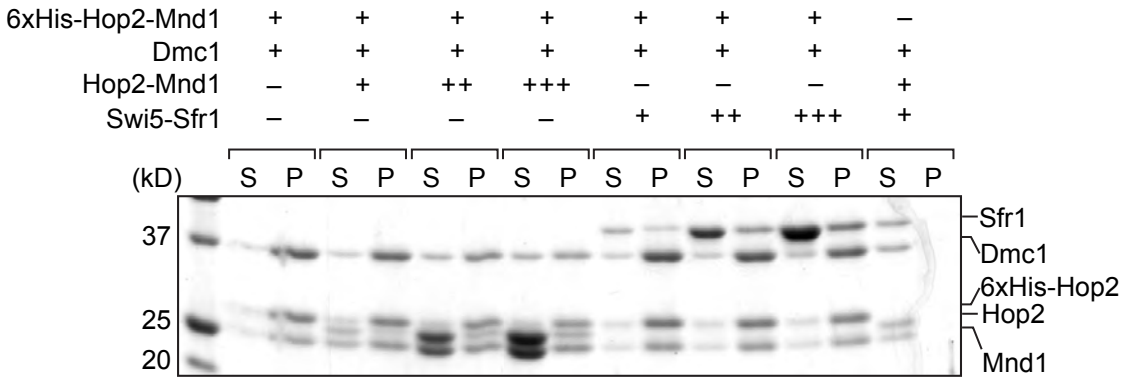
(A) Schematic of the dsDNA capture assay.

(B) css (PhiX174 virion DNA) annealed to a biotinylated oligo was initially incubated with the indicated proteins, then further incubated with linear dsDNA (ApaLI-digested PhiX174 RF I or BamHI-digested pBluescript KS^+). css was precipitated with streptavidin-coated magnetic beads and, after deproteinization, DNA in the supernatant (S) and the pellet (P) was analyzed by agarose gel electrophoresis. Quantitative data are shown in the graph where the supernatant and the pellet signals were combined and set at 100%. The percentage of the pellet signal to the sum was presented as dsDNA pulldown efficiency. Mean values ± SD from three independent experiments are shown.

A


+Dmc1
+Rad51
+Swi5-Sfr1
+RPA
6xHis-Hop2-Mnd1
– + – + – + – +
S P S P S P S P S P S P S P S P
Rad51
Dmc1
6xHis-Hop2
Mnd1
Rfa1
Sfr1
Rfa2
Rfa3
Swi5

B


6xHis-Hop2-Mnd1 + + + + + + + –
Dmc1 + + + + + + + +
Hop2-Mnd1 – + ++ +++ – – – +
Swi5-Sfr1 – – – – + ++ +++ +
(kD)
S P S P S P S P S P S P S P S P
37
25
20
Sfr1
Dmc1
6xHis-Hop2
Hop2
Mnd1

C

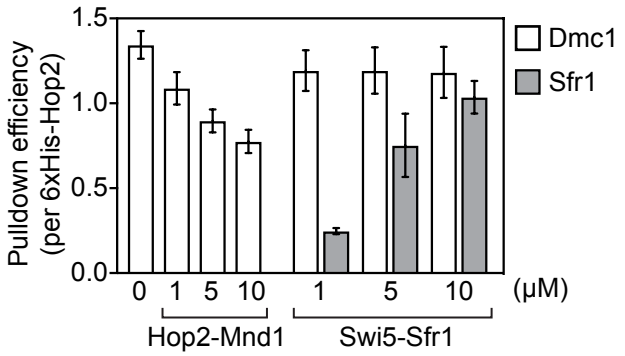

Pulldown efficiency
(per 6xHis-Hop2)
1.5
1.0
0.5
0.0
Dmc1
Sfr1
0 1 5 10 1 5 10 (μM)
Hop2-Mnd1
Swi5-Sfr1

Fig. S3. Hop2-Mnd1 and Swi5-Sfr1 likely bind to different interfaces of Dmc1.

(A) The interaction of Hop2-Mnd1 with proteins used in this study was examined by the pull-down assay. 6xHis-tagged Hop2-Mnd1 and the indicated proteins were incubated at 30˚C, mixed with Ni-conjugated magnetic beads, then the beads were separated from the supernatant (S) and proteins bound to the beads were eluted by heat-denaturing in the presence of SDS (precipitate, P). All the proteins were used at 3 μM.

(B) The interaction of 6xHis-Hop2-Mnd1 with Dmc1 was examined in the presence of various concentrations of either untagged Hop2-Mnd1 or Swi5-Sfr1 by the pull-down assay. The mixture of 6xHis-Hop2-Mnd1 and Dmc1 and the indicated proteins were incubated at 30˚C, mixed with Ni-conjugated magnetic beads, then the beads were separated from the supernatant (S) and proteins bound to the beads were eluted by heat-denaturing in the presence of SDS (precipitate, P). +, 1 μM; ++, 5 μM; +++, 10 μM.

(C) Pulldown efficiency assayed in (B) was expressed as the ratio of signal for the pulled-down Dmc1 or Sfr1 per the signal for the pulled-down 6xHis-Hop2. Mean values ± SD from three independent experiments are shown.

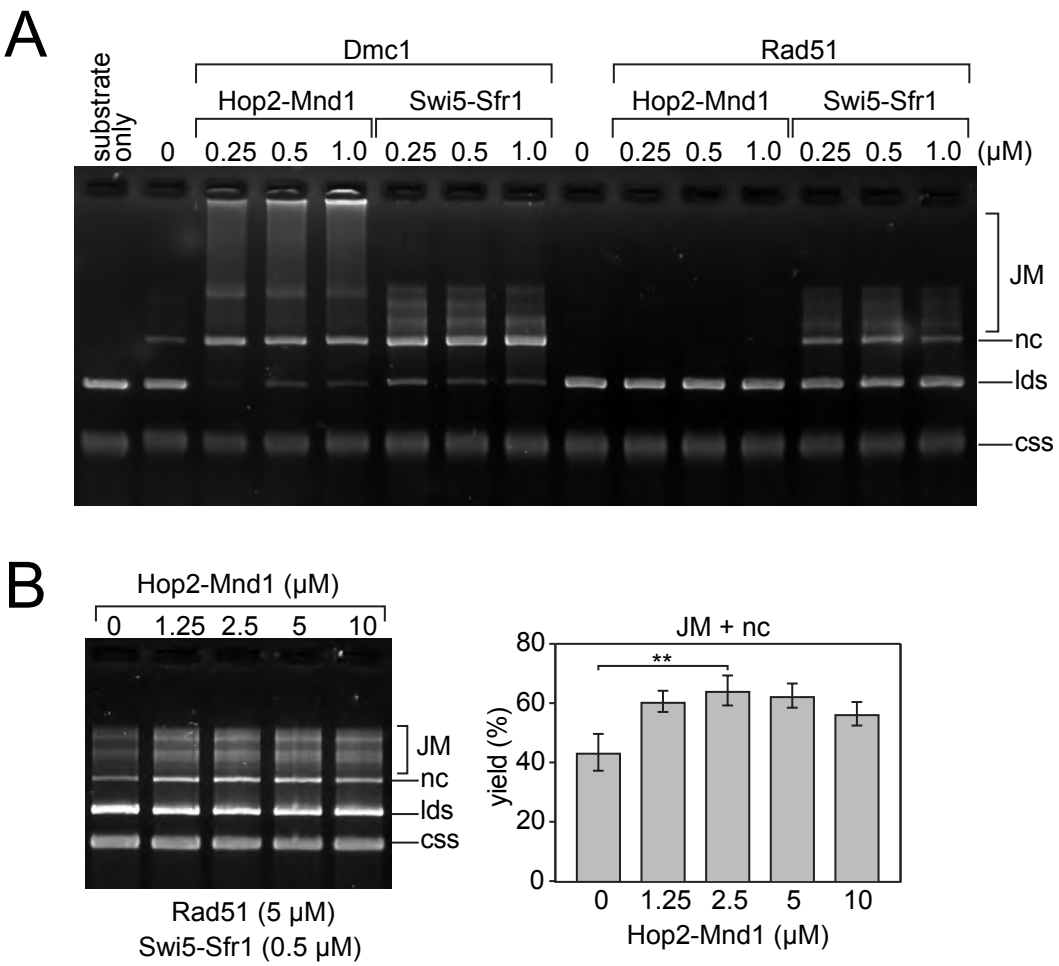
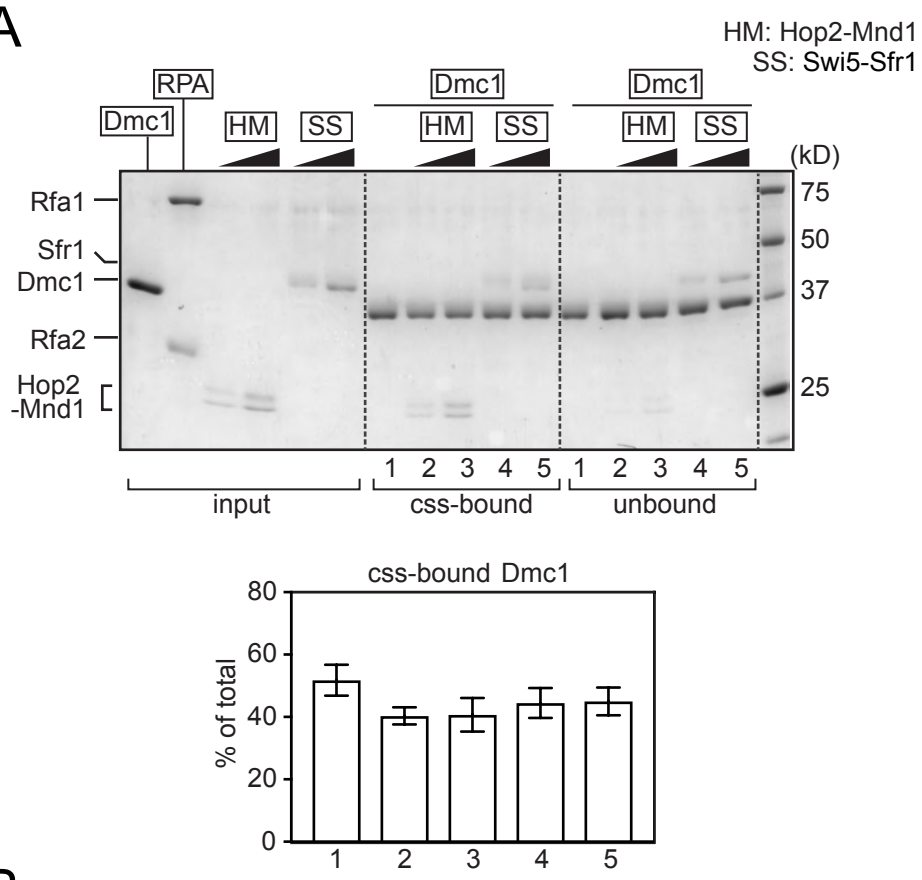

A
substrate only
Dmc1
Rad51
Hop2-Mnd1
Swi5-Sfr1
Hop2-Mnd1
Swi5-Sfr1
0
0.25 0.5 1.0
0.25 0.5 1.0
0
0.25 0.5 1.0
0.25 0.5 1.0
(μM)
JM
nc
lds
css
B
Hop2-Mnd1 (μM)
0 1.25 2.5 5 10
JM
nc
lds
css
Rad51 (5 μM)
Swi5-Sfr1 (0.5 μM)
JM + nc
**
yield (%)
80
60
40
20
0
0 1.25 2.5 5 10
Hop2-Mnd1 (μM)

Fig. S4. Hop2-Mnd1 weakly stimulates Rad51-driven strand exchange in the presence of Swi5-Sfr1.

(A) The effect of the indicated auxiliary factors on either Dmc1 or Rad51 was examined by the strand exchange assay. Rad51, 5 μM; Dmc1, 5 μM; RPA, 1 μM; css, 10 μM; lds, 10 μM.

(B) The effect of Hop2-Mnd1 on Rad51 in the presence of Swi5-Sfr1 was examined by the strand exchange assay. Mean values ± SD from three independent experiments are shown. **, $p = 0.0059$ (paired t-test). Rad51, 5 μM; Swi5-Sfr1, 0.5 μM; RPA, 1 μM; css, 10 μM; lds, 10 μM.

A



B

Swi5-Sfr1			Hop2-Mnd1		
conc. (μM)	k_{off} (s^{-1})	fold decrease	conc. (μM)	k_{off} (s^{-1})	fold decrease
0	0.25±0.0071	1.0	0	0.22±0.0072	1.0
0.15	0.054±0.00091	4.6	0.15	0.23±0.0068	0.96
0.3	0.037±0.00051	6.8	0.3	0.29±0.0092	0.76
0.6	0.028±0.00041	8.9	0.6	0.25±0.0071	0.88

Fig. S5. Further analysis of Dmc1 filament stability.

(A) css precoated with Dmc1 was incubated with the indicated auxiliary factor. css was precipitated with streptavidin-coated magnetic beads and associated proteins were examined (css-bound), along with proteins left in the supernatant (unbound), by SDS-PAGE. Mean values ± SD from three independent experiments are shown in the graph.

(B) Summary of dissociation rate constants obtained from the anisotropy assays shown in Figure 3D. Mean values ± SD from three independent experiments are shown.

SI References

1. R. Kintaka, T. Makino, H. Kitano, H. Moriya, K. Makanae, Identification of dosage-sensitive genes in Saccharomyces cerevisiae using the genetic tug-of-war method. *Genome Res.* **23**, 300–311 (2012).
2. N. Haruta, *et al.*, The Swi5-Sfr1 complex stimulates Rhp51/Rad51 - and Dmc1-mediated DNA strand exchange in vitro. *Nat. Struct. Mol. Biol.* **13**, 823–830 (2006).
3. Y. Kurokawa, Y. Murayama, N. Haruta-Takahashi, I. Urabe, H. Iwasaki, Reconstitution of DNA strand exchange mediated by Rhp51 recombinase and two mediators. *PLoS Biol.* **6**, 836–848 (2008).
4. N. Kuwabara, *et al.*, Mechanistic insights into the activation of Rad51-mediated strand exchange from the structure of a recombination activator, the Swi5-Sfr1 complex. *Structure* **20**, 440–449 (2012).
5. Y. Kokabu, *et al.*, Fission yeast Swi5-Sfr1 protein complex, an activator of Rad51 recombinase, forms an extremely elongated dogleg-shaped structure. *J. Biol. Chem.* **286**, 43569–43576 (2011).
6. J. Schindelin, *et al.*, Fiji: an open-source platform for biological-image analysis. *Nat. Methods* **9**, 676 (2012).